NIACINAMIDE ANALYSIS USING MOLECULARLY IMPRINTED POLYMERS

by

Reena Mistry

B.Sc., The University of British Columbia, 2008

A THESIS SUBMITTED IN PARTIAL FULFILLMENT OF

THE REQUIREMENTS FOR THE DEGREE OF

MASTER OF SCIENCE

in

THE FACULTY OF GRADUATE STUDIES

(Food Science)

THE UNIVERSITY OF BRITISH COLUMBIA

(Vancouver)

August 2012

Abstract

The objectives of this research were to use molecularly imprinted polymers (MIP) and microfluidic chips as an approach to a rapid and low cost analytical method for niacinamide analysis. Lab-on-a-chip (microfluidics) devices are becoming increasingly popular due to their relatively low cost, sensitivity, and speed. MIPs may be able to serve as solid-phase extraction packing material in microfluidic chips.

To reach the objectives, it was necessary to identify the mechanisms by which binding of analyte to polymer occur, determine the optimal functional monomer to cross-linker ratio, and gain an understanding of the polymeric structure and characteristic bonds. An MIP was created using niacinamide (NAM) as the template, methacrylic acid (MAA) as the functional monomer, ethylene glycol dimethacrylate (EGDMA) as the cross-linker, azobisisobutyronitrile (AIBN) as the free-radical initiator, and chloroform as the porogen. It was hypothesized that rebinding occurs via hydrogen-bonding of the carbonyl and amide groups of NAM to the oxygen atoms in the carboxyl group of MAA.

Rebinding studies were conducted using compounds with similar functional groups to NAM to determine binding mechanism to the polymer. Both the pyridyl nitrogen and the amide group were found to be important in hydrogen bonding interactions with the polymer.

Polymers were optimized for rebinding by using different ratios of functional monomer:cross-linker (MAA:EGDMA) and determining imprint factor of NAM to each polymer. The 1:4 polymer yielded the highest imprinting factor, indicating that the polymer is most selective for NAM.

FTIR was conducted to determine the structure of polymers created and whether NAM detection and quantification was possible. There was a peak at 1725 cm^{-1}, which was a shift of the C=O stretching band from 1694 cm^{-1} in MAA and 1717 cm^{-1} in EGDMA, indicating a chemical interaction between the two compounds. The disappearance of a peak at 1633 cm^{-1} showed a loss of conjugation in the carboxylic acid in the polymeric structure.

Through this research, knowledge was gained about the polymer optimization and structure. However, more studies need to be conducted to determine the feasibility of an MIP application for a lab-on-a-chip device.

Table of Contents

List of Tables

List of Figures

List of Equations

List of Symbols and Abbreviations

AIBN: Azobisisobutyronitrile

AOAC: Association of Official Analytical Chemists

CE: Capillary Electrophoresis

COMOSS: Collocated Monolithic Support Structures

CV: Coefficient of Variation

DCM: Dichloromethane

EGDMA: Ethylene Glycol Dimethacrylate

FTIR: Fourier-Transform Infrared

HPLC: High Performance Liquid Chromatography

MAA: Methacrylic Acid

MIP: Molecularly-imprinted Polymer

NIP: Non-imprinted Polymer

NAM: Niacinamide

PDMS: Polydimethylsiloxane

PMMA: Poly (methyl methacrylate)

RPM: Rotations per Minute

SEM: Scanning Electron Microscopy

SPR: Surface Plasmon Resonance

TRIM: Trimethylolpropane Trimethacrylate

UATR: Universal Attenuated Total Reflectance

Acknowledgements

I am first and foremost grateful to my parents for empowering me and supporting me to have a better life for myself, and teaching me that the sky is the limit. I would also like to thank my sisters and extended family members for supporting me in this journey.

I owe my deepest gratitude to Dr. Christine Scaman for giving me this opportunity to do a Master's of Science degree under her supervision, and whose guidance and support enabled me to develop an understanding of the subject. I would like to thank my committee members, Dr. Timothy Durance, Dr. Eunice Li-Chan, and Dr. Boris Stoeber for their counsel throughout this journey. Also, I am indebted to Valerie Skura, Pedro Aloise, Katie Du, Parastoo Yaghmaee and Benny Chan for their technical and analytical support throughout my research. I would also like to recognize the Vitamin Research Fund for financially supporting this work.

It was an honor to work alongside my colleagues, Andrea Goldson, Orly Varon, Venkatrao Konasani, and Alireza Riazi, without whose moral support I could not have done this. I would also like to recognize Rebecca Hartley, Charmaine Koo, and Magdalena Surma for their contributions to my research.

I thank all of my teachers at Umatilla High School in Oregon for believing in me and my success, and encouraging me to be the best I can be. I am especially grateful for my high school chemistry teacher, Mr. Ron Sehman, for inspiring me at a young age and helping me to discover my passion for chemistry.

And lastly, but not least, I would like to express my gratitude to my current employer, Daiya Foods Inc. for affording me the time to work on my thesis.

For my grandmothers,

the late Lalitaben Mistry &

Jasuben Gajjar,

who did not have the same opportunities I have today,

but set the path for my success.

Chapter 1. Introduction

Niacinamide (NAM) is one of the two principle forms of the essential nutrient vitamin B3, which is also known as niacin or vitamin PP. The other form is nicotinic acid. Some significant sources of niacin can be found in meat, eggs, fish, enriched grain products and nuts. NAM is especially important due to its role in the coenzyme formation of nicotinamide adenine dinucleotide (NAD) and nicotinamide adenine dinucleotide phosphate (NADP), which are important for metabolism of living cells. Pellagra is a disease caused by a niacin deficiency and is characterized by symptoms such as, but not limited to, diarrhea, dementia, and dermatitis, and can lead to death. However, the intake of too much niacin can also cause niacin toxicity in the body, as in the acid form it competes with uric acid for excretion and can cause gouty arthritis. The amide form is 2-3 times more toxic than nicotinic acid. Therefore, there is a need for analytical techniques to measure the amounts present in foods or supplements.

Polymers are large high molecular weight molecules (macromolecules), which are comprised of smaller molecular weight components called monomers. The monomers impart functionality to the polymer, which can then influence the overall properties of the final polymer. Molecular imprinting is a method by which highly selective recognition sites can be generated in a synthetic polymer using a template to yield molecularly imprinted polymers (MIPs). MIPs, which are extensively cross-linked polymers, contain specific recognition sites with a pre-determined selectivity for a chosen analyte based on a template (Holland 2008).

The template, which may be the target molecule, interacts with functional monomers to form complexes using covalent or non-covalent interactions. This template-monomer complex is then polymerized in the presence of a cross-linking monomer and a porogen, which is a solvent. The polymerization acts to hold the template within a rigid polymer matrix. Template removal leaves an available recognition site with high affinity for the target molecule. The shape and size of the imprint (or recognition/binding site) and the spatial arrangement of the functional groups are complementary to the structure of the template molecule (Holland 2008).

MIPs have been widely researched for use in solid phase extraction applications (Beltran and others 2010), as well as for use as controlled-release drug delivery systems (Del Sole and others 2007; Del Sole and others 2010). More research needs to be conducted to ascertain fundamental knowledge on formation and utilization, including, but not limited to, determining the mechanisms by which the interactions between the target molecule to MIP occur, which are involved in determining pore sizes, particle formation, and rebinding. Additionally, it has been noted that the ratio between the functional monomer and cross-linker play a role in the rebinding efficacy of the target molecule to the MIP (Del Sole and others 2010).

In this study, a MIP was created based on a method published by Del Sole and others (2010), using MAA as the functional monomer, EGDMA as the cross-linker, NAM as the template, chloroform as the porogen, and AIBN as the free-radical initiator. MIPs were created with different MAA:EGDMA ratios to understand the effect of cross-linker on the polymer characteristics and target molecule (NAM) rebinding, as well as to gain an understanding of the structure of the molecule. Rebinding studies were

conducted with structurally-related molecules that exhibit select functionalities similar to the NAM molecule to determine which functional group of NAM is important for affinity to the MIP. Polymers were analyzed for further chemical and physical characteristics with FTIR and scanning electron microscopy (SEM) images. The results from this work provide insights for future development of NAM-imprinted polymers, as well as analytical applications for MIPs.

Chapter 2. Research Hypotheses and Objectives

The purpose of this study was to develop a suitable MIP for niacinamide as the template and determining its binding characteristics to the template/analyte.

2.1. Research Hypothesis

1) There will be an optimal monomer to cross-linker ratio, using MAA as the functional monomer and ethylene glycol dimethacrylate (EGDMA) as the cross-linker, that is most selective for NAM rebinding studies.
2) Niacinamide (NAM) binding to MIP occurs primarily via hydrogen bonding with the amide group in the NAM to the carbonyl group in the methacrylic acid (MAA).
3) FTIR could serve as a potential analytical tool for NAM quantification in polymers, as well as determine characteristic bonds in the final polymeric structure of the MIP and NIP.

2.2. Research Objectives

1) Identify the optimal functional monomer to cross-linker ratio (MAA:EGDMA) for NAM selectivity during rebinding studies.
2) Conduct rebinding studies with molecules that exhibit select functionalities similar to the NAM molecule —pyridine, benzamide, and acetamide—to help understand the mechanism by which NAM binds to the MIP in the polymer made according to the method used by Del Sole and others (2010).

3) Determine characteristic bonds of the polymeric structure of the MIP, and of the polymer-bound NAM using Fourier transform infrared spectroscopy (FTIR) methods.

Chapter 3. Literature Review

3.1. Niacinamide

Vitamin B3, also known as niacin, is a water-soluble vitamin comprised of two chemical forms: nicotinic acid and niacinamide (also known as nicotinamide) (Figure 1).

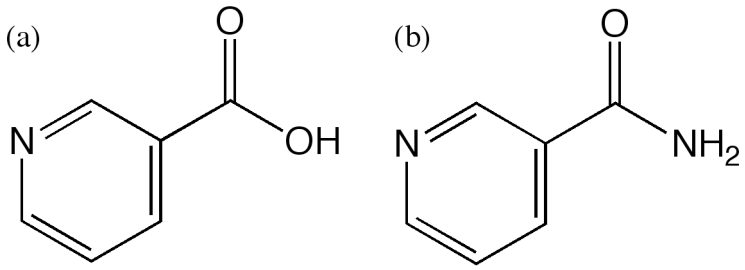

Figure 1. Chemical structures of nicotinic acid (a) and niacinamide (b)

Niacin deficiency is called "pellagra" and was first noted in 1735 in Spain (Stratigos and Katsambas 2006). However, it was not recognized as a nutritional deficiency until 1920. Pellagra is characterized as the "three D's disease" because it has the symptoms of dermatosis, dementia, and diarrhea. In 1937, nicotinic acid was recognized as the key factor in curing pellagra. Biochemically, nicotinic acid and niacinamide (NAM) serve as the precursors for the synthesis of NAD and NADP. The metabolically active form of the coenzymes is NAM, which is also the primary circulating form of niacin. NAD and NADP function in redox reactions, in which NAM acts as an electron acceptor or hydrogen donator (Eitenmiller and Landen Jr. 1999).

NAM has higher solubility in water (100g/100 ml) than nicotinic acid (1.67 g/100 ml). It is the most stable water-soluble vitamin. Thermal processing, light, acid, alkali, or oxidation does not affect its biological activity. Both acid and amide show similar

absorption properties, with the absorption maxima near 260 nm (Eitenmiller and Landen Jr. 1999).

3.2. Methods for Niacinamide Analysis and Detection

Several methods exist currently for the analysis of niacin and niacinamide, many of which are official AOAC (Association of Official Analytical Chemists) methods. The colourimetric method (AOAC 961.14) is commonly used for niacin and niacinamide determination in drugs, foods, and feeds, whereas the spectrophotometric method (AOAC 968.32) is only for multivitamin preparations. The microbiological method (AOAC 944.13) is also for vitamin preparations, while the microbiological-turbidimetric method (AOAC 985.34) is only for ready-to-feed milk-based infant formula.

3.2.1. AOAC Official Methods for Niacin Analysis

The AOAC official methods for niacin and niacinamide colorimetric analyses (AOAC 961.14) use the König reaction (Eitenmiller and Landen Jr. 1999). In the König reaction, the heterocyclic nitrogen of the pyridine group reacts with cyanogen bromide and is then coupled with an aromatic hydrocarbon containing an amine group to give a dye polymethine (Capella-Peiró and others 2004). In this assay, the cyanogen bromide is reacted with sulfanilic acid. The sample preparation of the method involves extracting niacin with acid and then adjusting the pH to 4.5 with a base. Samples must be clarified by heating and cooling, followed by centrifugation or filtration. After samples are prepared, the multistep reaction takes place in a larger cuvette and is read against a blank reaction in a spectrophotometer between 430 and 450 nm for pharmaceutical preparations and noncereal foods and feeds, and at 470 nm for cereal products. The limits of detection are not stated in the official method. However, it is able to detect niacin in a cereal

product at 40 µg/g and 35 µg/g in noncereal foods and feeds and pharmaceutical applications (Association of Official Analytical Chemists International 1998a).

For multivitamin samples that are significantly higher in niacinamide than niacin (by at least 3 times), the AOAC Method 968.32 was developed. The reaction is much simpler as it only requires a manual grinding of multivitamins and dissolution and is specific for niacinamide. This method also involves the König reaction because it requires the use of cyanogen bromide with barbituric acid, which is also an aromatic hydrocarbon containing an amine group. The colour formation has a maximum absorbance at 550 nm on the spectrophotometer and samples are quantified using a standard curve (Association of Official Analytical Chemists International 1998d).

Subsequent automated colorimetric AOAC methods developed for niacin analysis in cereals involved using in-line dialysis for the last clarification step, replacing the $(NH_4)_2SO_4$ precipitation, and was based on the Technicon AutoAnalyzer II system (Association of Official Analytical Chemists International 1998b). For noncereal foods, drugs, and noncereal feeds, a general automated method was implemented after the automated method for cereals (Association of Official Analytical Chemists International 1998c). It was determined that both of the automated AOAC methods for niacin determination are more precise than the manual method (Method 961.14). In addition, due to higher sample throughput, labour and analysis time are decreased (Eitenmiller and Landen Jr. 1999). However, these methods still involve several chemicals and steps for the assay, and still allow some room for error. Additionally, the sample sizes needed are still fairly large for the sample preparation.

The official AOAC microbiological method for niacin and niacinamide analysis (method 944.13) can be approached titrimetrically or turbidimetrically. For the titrimetric method, samples are inoculated using a purified *Lactobacillus plantarum* culture (Association of Official Analytical Chemists International 1998e). The inoculum responds on a molar basis to nicotinic acid, NAM, and NAD and can reliably measure total niacin in biological and pharmaceutical samples (Eitenmiller and Landen Jr. 1999). The prepared sample solutions of foods or multivitamins that contain NAM, nicotinic acid, or NAD are titrated with 0.1N NaOH, using bromothymol blue indicator, or to pH 6.8 if measured potentiometrically. Niacin content is determined with a standard curve (Association of Official Analytical Chemists International 1998e). The turbidimetric method is similar. An inoculum of *L. plantarum* is added to the sample and standards, which are incubated for 16-24 hours until maximum turbidity is obtained. The turbidity is measured with a photometer with a wavelength between 540 and 660 nm (Association of Official Analytical Chemists International 1998f). Sensitivity and limits of detection were not discussed in the official AOAC microbiological methods. One limitation to the microbiological methods is that it takes time for the microorganisms to react with NAM and culture the cells. Additionally, this is not a direct method of determination of niacinamide, leading to potential errors or false positives, and potentially a lower sensitivity.

3.2.2. HPLC and Capillary Electrophoresis Methods for Analysis

There are many papers discussing high-performance liquid chromatography (HPLC) and capillary electrophoresis (CE) methods for niacinamide analysis. Discussed here will be general principles of the methods and a few specific applications. HPLC is a liquid chromatography analyte separation method improved with the additions of pumps,

injection valves, and detectors. It can be applied to any analyte that is soluble in a liquid that can be used as a mobile phase (Reuhs and Rounds 2010).

The basic components of an HPLC system involve a pump, injector, column, detector, and a data system. The HPLC pump delivers the mobile phase, which is the solvent carrying the analyte through the stationary phase in the column. The pump can flow the mobile phase through in a controlled, precise, and accurate measure at a constant flow rate. The injector, typically a valve injector, places the sample into the mobile phase on the column in a precise manner at a specified injection volume. The column houses the stationary phase through which the analytes are separated and they are typically 10-25 cm in length with an internal diameter of 4.6-5 mm. An analytical column requires a guard column in front of it as a sample clean up procedure. The guard columns protect the analytical column from strongly adsorbed sample components. A detector is placed at the end of a column and translates the changes in sample concentration into an electrical signal. Detectors can be spectroscopic, electroanalytical, light scattering, radioactive detectors, nitrogen detectors, or even be coupled with other analytical techniques for detections such as mass spectrometry (MS) or nuclear magnetic resonance (NMR). The detection method used depends highly on the type of analyte being measured (Reuhs and Rounds 2010).

The use of HPLC methods for niacin measurement has been criticized because it is necessary to use UV detection. This is criticized because the wavelength that niacinamide absorbs at (262 nm) is one that many compounds can absorb, potentially leading to interference. UV detection is suitable for high concentration vitamin samples, but as it is not very specific it can often result in chromatograms with unresolved

interferences. LC methods for biological samples that utilize UV detection must include clean up procedures for the removal of interfering compounds (Eitenmiller and Landen Jr. 1999).

The poor resolution of niacin due to the use of UV detection has led to investigations of the development of complex chromatographic systems, in addition to the use of extensive extract purification methods. Ion-pair chromatography, such as tert-butylammonium hydroxide or sodium dodecyl sulfate, can improve the resolution of niacin from interfering peaks. Another approach to improving the detection of niacin after LC resolution utilizes a post-column derivatization technique that involves the detection of a chromophore developed by the König reaction with potassium cyanide, as opposed to cyanogen bromide used in the AOAC methods. This led to chromatograms, having low baseline noise, with high specificity for nicotinic acid and NAM (Stein and others 1995).

Capillary electrophoresis is visually similar to HPLC in terms of set up because of the programmable samplers, separation columns, separation buffers, and detection devices. However, it differs from HPLC in two significant ways. The first is the injection type and liquid flow within the capillary. In HPLC, injection volumes are dependent on the syringe volume or injection loop size. In CE, the hydrodynamically injected volumes are directly dependent on the size and type of the separation capillary. The second is that unlike HPLC, the buffer velocity is not pressure driven, but is rather electrokinetically governed by the electroosmotic flow induced by quality of the capillary surface, thereby separating analytes by charge (Schmitt-Kopplin and Fekete 2007).

CE has been used for analyzing niacinamide in food samples. Ward and Trenerry (1997) used alkali extraction of their samples, as well as purification and concentration with solid-phase extraction on a Sep-Pak C_{18} and SCX cation exchange columns connected in sequence, to achieve comparable results to HPLC for niacin determination in various foods, including, but not limited to, cereals, meat, fish, peanut butter, and sunflower seeds. The CE used a 75 μm uncoated, fused silica capillary column with acetonitrile:phosphate buffer pH 7.0 (15:85). Detection was at 254 nm, and the chromatograms were reportedly cleaner than with HPLC. The method was also faster and had a lower sample cost (Ward and Trenerry 1997).

The above methods all require extensive steps in the sample preparation procedures, such as extraction or sample purification, typically involving a pre-column clean up step. Furthermore, specificity for the HPLC methods has been questioned, as mentioned, due to the detector. MIP technology may provide a faster, more specific alternative for niacin analysis that can potentially require less extensive clean up steps.

3.3. What are Molecularly-Imprinted Polymers?

Molecular imprinting is a synthetic approach to mimic natural chemical recognition by preparing substrate-selective recognition sites in a matrix using a molecular template in a casting procedure. As can be seen in Figure 2, the template molecule first forms interactions or bonds in a solution with one or several types of functional monomers as a preassembly step. Then these interactions/bonds are subsequently "locked-in" by the formation of a matrix around them, and as a result then have specific recognition sites selective for the template, like a lock and key as shown in Figure 2 (Ramstrom 2005a).

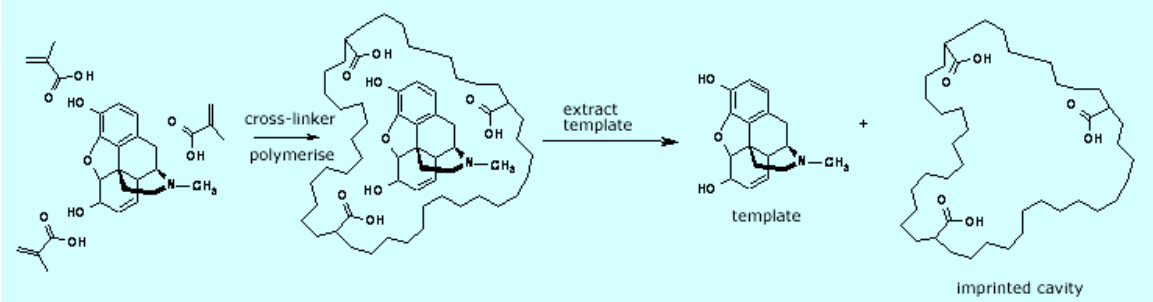

Figure 2. Schematic diagram of preassembly, polymerization, and template extraction during MIP synthesis (Mayes Research Group n.d.).

There are three approaches to molecular imprinting—non-covalent, covalent, and semi-covalent (which is a combination of the first two). In the non-covalent approach, a complex is first formed between the template molecule and the functional monomer that possesses complementary functional groups to those of the template using weak non-covalent interactions. Then the cross-linking monomers are added and the mixture is polymerized to permanently fix the spatial arrangement of the functional monomers. The template is extracted after polymerization, and the empty cavities left behind are complementary in size, shape, and chemical functionality to the template molecule. These cavities can then selectively and reversibly bind molecules that are identical or very similar to the original template using non-covalent bonds such as van der Waals forces, ionic interactions, hydrogen bonds, and hydrophobic interactions (Yilmaz and others 2005).

The covalent approach involves formation of reversible covalent bonds between the template and monomer before polymerization. The template is removed via cleavage of corresponding covalent bonds, which are formed again when the analyte is rebound to the polymer (Wulff 2005). The template is covalently bound to an appropriate stoichiometric amount of functional monomer in the pre-polymerization mixture.

Therefore, once the MIP is polymerized there is no issue of having excess monomer, resulting in all of the functional groups in the imprinted polymer being present in the imprint sites only, and in precise homogeneous spatial arrangement for rebinding, minimizing the existence of non-specific binding sites present in non-covalent MIP synthesis methods. While this seems like an ideal template-monomer situation, the range of template functionality for which efficient reversible complex formation is possible is very limited (Kirsch and Whitcombe 2005; Tamayo and others 2007).

As touched on in the previous paragraphs, each method for synthesizing MIPs has their advantages and disadvantages. The non-covalent approach is the simplest method and has broad applications to a range of template structures. It is relatively inexpensive and requires less specialist knowledge in polymer chemistry to prepare MIPs with good selectivity and high affinity for the template. However, its main disadvantage is that it requires the use of excess functional monomer to form the pre-polymerization complexes, which leads to a large number of distributed functional monomer unit that are not associated with a template, contributing to a higher amount of non-specific binding (Yilmaz and others 2005). Furthermore, the dynamic nature of the template-monomer interactions in non-covalent approaches creates a distribution of binding sites with different affinities for the template (Kirsch and Whitcombe 2005). As mentioned previously, the covalent approach for MIP synthesis does not suffer from any of the problems of using an excess of functional monomer since the template covalently binds to a stoichiometric amount of functional monomer in the pre-polymerization mixture. This leads to a polymer with all functional groups in precise spatial arrangement for rebinding. The biggest drawback to this method is the limited range of template

functionality for which efficient reversible covalent complex formations are possible. Most covalent interactions are too stable to be cleaved and too slow to be rebound in the reversible interaction. A further drawback of this method is that it can sometimes involve complicated syntheses of the binding monomers (Wulff 2005).

The semi-covalent approach combines the advantages of both methods by the polymerization of a template that is covalently bound to a functional monomer by a cleavage linkage. Template removal, occurring by hydrolysis, leaves an imprint with functional groups that are capable with interacting with the template in a non-covalent manner during the rebinding step. Therefore, the resulting polymer would have all of the functional groups that were introduced in the imprinting step associated with an introduced template. The functional groups also would not be randomly distributed because no excess monomer would be used, leaving the binding sites more uniform in nature. Additionally, the template that is not removed in the hydrolysis step would remain covalently bound to the polymer and would not therefore contribute to template "bleeding" that can occur in non-covalently imprinted polymers. The main disadvantage to the semi-covalent approach to MIP synthesis is the need for specialist knowledge to design and synthesize a suitable template and polymer with reversible covalent linkages. And for this reason, non-covalent approaches are still most widely accepted for MIP syntheses (Kirsch and Whitcombe 2005). Promising interactions for MIP synthesis are non-covalent with high association constants between the template and the binding site. A summary of the general advantages and disadvantages can be found in Table 1.

Table 1. Advantages and disadvantages of non-covalent, covalent, and semi-covalent MIP synthesis approaches (Kirsch and Whitcombe 2005; Wulff 2005; Yilmaz and others 2005; Tamayo and others 2007)**.**

	Non-covalent	**Covalent**	**Semi-Covalent**
Choice of template and functional monomer	*Wide variety*	Restricted to templates and functional monomers with appropriate reversible covalent functionalities	Restricted to templates and functional monomers with appropriate reversible covalent functionalities
Preparation of MIP	*Easy and straightforward*	Preparation of covalently bound pre-polymerization complex necessary	Preparation of covalently bound pre-polymerization complex necessary
Polymerization conditions	Critical; only non-covalent interactions govern the pre-polymerization complex (less stable)	*Less critical; pre-polymerization complex is more stable*	*Less critical; pre-polymerization complex is more stable*
Affinity of binding sites	Heterogeneous	*Homogeneous*	*Homogeneous*
Selectivity for template	Lower selectivity	*Higher selectivity*	*Higher selectivity*
Removal of template after polymerization	*Easy, uses mild conditions*	Cleavage of the covalent monomer-template linkage is necessary	Cleavage of the covalent monomer-template linkage is necessary
Rebinding kinetics	*Fast*	Slow	*Fast*

3.3.1. Templates

Templates are the most important part of the MIP as it functions to direct the monomers to form the imprinted shape. The template is typically the analyte you are trying to measure or quantify using the MIP, but sometimes an analogue molecule is used in place of the analyte. This is because not all templates can be imprinted into polymers, however. Ideally, a good template needs to be chemically inert under the polymerizing conditions. If a template can participate in radical reactions or is unstable for other reasons under polymerizing conditions, alternative strategies for imprinting should be investigated. The following questions should be asked when selecting a template: 1) Does the template have any polymerisable groups? 2) Does the template have functionality that may potentially inhibit or delay free radical polymerization, such as a

thiol group or hydroquinone moiety? 3) Is the template unstable at moderately elevated temperatures, such as 60ºC if AIBN is used as the free-radical initiator, or upon exposure to UV irradiation? If the answer to these questions are "yes," then alternative approaches (methods and/or templates) should be explored (Cormack and Elorza 2004).

3.3.2. Functional Monomers

There are two main types of building blocks used for creating MIPs—functional elements and structural components. Functional elements are typically those monomers that directly associate with the template or target species. Structural components are monomers, whose main functions are organization, shape, and overall structure of the polymer. Typically, in MIP terminology, these are called functional monomer and cross-linkers, respectively (Ramstrom 2005b).

Functional monomers can be divided into three major groups, which depend on whether the protocol makes use of general noncovalent interactions, metal-coordination, or reversible-covalent protocols. The noncovalent group can be further divided into subgroups, depending on the major interaction in the group, such as acidic, basic, hydrogen bonding, or even dipole-dipole stacking. Functional monomers can also be grouped based on if they are broad-spectrum monomers or specific monomers, depending on the specificity to certain templates. In general, the more functionally complex a monomer is, the more specific it becomes. Functional monomers capable of forming multiple noncovalent interactions with the template will lead to stronger complexations and potentially higher binding strength in the binding site within the polymer (Ramstrom 2005b).

Typically, functional monomers are used in excess compared to the template, involving a 1:4 or lower template:monomer ratio. It is important that the functional

monomer chosen should have a functionality that complements the functionality of the template. For example, a hydrogen bond donor should match with a hydrogen bond acceptor (Cormack and Elorza 2004). Common functional monomers include, but aren't limited to, methacrylic acid (noncovalent), 4-vinylphenylboronic acid (reversible covalent), *N*-vinyl-2-pyrrolidinone (noncovalent), and acrylamide (noncovalent) (Ramstrom 2005b).

3.3.3. Cross-linkers

Cross-linking monomers have two or more polymerizable groups and comprise the bulk mass of the imprinted polymer. They can be chosen to increase the selectivity of the imprinted site, especially in noncovalent protocols (Ramstrom 2005b). Cross-linkers, however, have three main roles in the MIP. The first is that it controls the morphology of the polymers, dictating whether it is a gel-type, macroporous, or a microgel powder. Secondly, it serves to stabilize the imprinted binding site. The third role is to mechanically stabilize the entire polymer matrix. It is typical for the cross-linker to comprise 80% or more of the polymer, which is important to give it a permanent macroporous structure, allowing the imprinted site to be available. When choosing a cross-linker, the reactivity ratio of the compound should be matched with the functional monomer in order for them to be copolymerized (Cormack and Elorza 2004).

The most popular cross-linker used for MIPs is ethylene glycol dimethacrylate (EGDMA), which is used in many protocols involving acrylate or acrylamide functional monomers. Trimethylolpropane trimethacrylate has recently become popular as well, as it has been proven superior in some cases. Divinylbenzene is a common cross-linker for styrene-based protocols. None of these cross-linkers are water-soluble. Therefore, organic porogens, which are described in section 3.3.4, are commonly used. The most

common cross-linker used for MIP made with water or alcohol is 1,4-bis(acryloyl)piperazine, which is easily soluble in both porogens at high concentrations (Ramstrom 2005b).

3.3.4. Porogens

A porogen is the solvent in which the MIP or NIP is created. The porogen aids in creating the pores in the polymer, hence its name. The choice of porogen is critical for obtaining a good imprint, as well as for successful rebinding or template recognition. It is important that the solvent dissolves all of the components in the prepolymerization mixture because this allows for optimal template-monomer interaction, and contributes to good porosity characteristics of the final polymer. For most MIPs, aprotic organic solvents with low polarity are most ideal for achieving good imprints. This is because highly polar aprotic solvents, such as dimethylformamide (DMF), can interfere with ionic and van der Waals forces between the template and functional monomer. Protic solvents, such as water or methanol, can interfere with hydrogen bonding (Yilmaz and others 2005).

The porogenic solvent plays an important role in the pore size distribution of an MIP. Larger pores can be obtained in poorer solvent because the onset of phase separation occurs earlier. During polymerization, the growing polymer chains precipitate out of solution either because of extensive cross-linking or because their molecular weights have exceeded the solubility limit of the porogen. If a poor solvent is used, phase separation occurs earlier and the nuclei formed as a precursor to the polymer swells with monomers, leading the polymeric globules that form to be larger. Therefore, the voids between each globule of the polymer are also larger. Alternatively, if a good solvent is used for MIP formation, it will compete with the monomers to solvate the

nuclei. Thus, the monomer concentration within the nuclei is smaller. The nuclei tend to not swell as much, leading to smaller globules and smaller pores overall (Brazier and Yan 2005).

Another parameter that can be considered when choosing a porogen is the solvent's dielectric constant, which is important for electrostatic forces between two charged entities. The binding strength between two oppositely charged molecules in solvents with low dielectric constants, such as toluene, is high. Alternatively the binding strength is decreased significantly in polar solvents, such as water or DMF, because they are potent in breaking hydrogen bonds or salt bridges (Yilmaz and others 2005).

Finally, the hydrogen bond parameter (HBP) of a solvent should be considered when choosing the right porogen. HBP denotes the ability of a solvent to form hydrogen bonds with molecules of the same kind or with solutes. A solvent with high HBP will easily dissolve polar molecules able to create hydrogen bonds, but will also interfere with the hydrogen bonds formed between the functional monomer and template, leading to MIPs with lower selectivity. High HBP solvents disturb the template-monomer complex, leading to MIPs with lower affinity binding sites. Typical porogens used for imprinting small molecules include toluene, acetonitrile, and chloroform (Yilmaz and others 2005).

3.3.5. Free-radical Initiators

Many different free-radical initiators can be used in a free-radical polymerization. Based on their chemical nature, the rate and mode of decomposition of an initiator to radicals can be triggered and controlled in a number of ways, including heat, light and by chemical/electrochemical means. While almost any free-radical initiator can be used to drive a polymerization in the presence of templates, there are advantages to using some over others. For example, if the template were thermally or photochemically unstable,

then initiators that can be triggered thermally and photochemically, respectively, would not be desirable. When hydrogen bonding drives monomer complexation, then lower polymerization temperatures are preferred. In such cases, a photochemically active initiator may be more preferred as they can operate effectively at lower temperature (Cormack and Elorza 2004). Typical initiators include AIBN (Del Sole and others 2010), benzoyl peroxide (Mookda and others 2008), azobisdimethylvaleronitrile (ABDV), and 4,4′-azo(4-cyanovaleric acid) (Cormack and Elorza 2004).

3.4. Previously Reported Methods for Niacinamide-Imprinted Polymers

One of the first mentions of niacinamide-imprinted polymers is by Fu and others (2001). Their research comprised of determining template recognition characteristics for polymers created with different porogens and different templates including NAM and its positional isomers. MIPs were created and analyzed by packing into an HPLC column and comparing chromatograms and retention times. Templates used to create the polymer were NAM, isonicotinamide, and picolinamide. Porogens used were chloroform and acetonitrile. Functional monomers studied were MAA and acrylamide. MAA was selected because it has the ability to interact with both the amide group and the heterocyclic nitrogen from NAM using the carboxylic acid group, and it was shown that the polymers created with MAA generally had higher binding capacity factors (κ') than with acrylamide. This was ascribed to the stronger hydrogen-bonding interaction between the acidic MAA monomer and the alkaline NAM template (Fu and others 2001).

It was found that isonicotinamide and NAM were able to bind strongly to their respective MIPs. Interestingly, it was also shown that isonicotinamide was also able to bind more strongly to NAM MIP than it was able to bind to the NIP. This indicates that

there is relatively low specificity of the MIP to structurally similar compounds. On the other hand, picolinamide showed a poorer overall κ'on all the polymers tested, which was ascribed to the intramolecular hydrogen bond between the heterocyclic nitrogen and the amide group reducing its binding to the MIP (Fu and others 2001).

Fu and others (2001) also showed that the use of different porogenic solvents influence the MIP formation. They made polymers with acetonitrile and chloroform and compared the binding characteristics of each. It was shown that the κ' of the polymers made with chloroform, which is more non-polar, were generally higher than that of the polymers made with acetonitrile, which is more polar. Thus, they confirmed that non-polar solvents favor the interaction of the monomer and template in this case (Fu and others 2001).

Finally, this research group was also able to show the selective binding for nicotinic acid and isonicotinic acid with their respective amide MIP. The acid counterparts had a stronger κ' than the amides, proving that the template recognition can persist in the acid system. This is noteworthy, because, as they pointed out, nicotinic acid has low solubility in chloroform (the ideal porogen) and thus, its amide can be used as a template instead (Fu and others 2001).

In 2003, the same research group developed a computational approach for simulating the synthesis of molecularly imprinted polymers using NAM as a template (Wu and others 2003). They determined that the higher the interaction energy of the template to functional monomer, the higher the binding energy. In general, this computer modeling system demonstrated the relationship of the template and functional monomer, and it was suggested to be useful for finding an appropriate functional

monomer for a given template, as well as for demonstrating template and analogue behaviour on a given MIP (Wu and others 2003; Wu and Li 2004).

The one limitation to their computer modeling system was that it did not take into consideration the effect on polymerization and binding capacity by the porogenic solvent used (Wu and others 2003; Wu and Li 2004). As mentioned earlier, porogens play a role in affinity and selectivity for the template and rebinding analyte by the MIP (Brazier and Yan 2005; Yilmaz and others 2005). This problem was solved later on by conducting theoretical computational studies and validating empirically using NAM MIPs with different porogens (Wu and others 2005). This is different from their previous study, as they had only tested MIP formation with acetonitrile and chloroform (Fu and others 2001). It was shown that when porogens with a strong capacity to form hydrogen bonds are used, such as methanol, the interference from the hydrogen bonding affects the formation of the template-monomer complex and the interaction energy between the functional monomer and template. In contrast, when an aprotic porogenic solvent is used, which has a smaller dielectric constant, the interaction energy between the template and functional monomer was larger. This favors the formation of a larger concentration of template-monomer complexes in the prepolymerization mixture, thus resulting in a MIP with a high degree of selectivity and affinity. For an aprotic porogen system, only the porogenic dielectric constant needs to be considered for MIP formation. Conversely, for a protic porogen, both dielectric constant and hydrogen bonding interference of the porogen need to be considered (Wu and others 2005). This study further supported their earlier findings (Fu and others 2001).

Zhang and others (2005) conducted binding studies with different concentrations of niacinamide to understand the adsorption characteristics of the polymers formed with different ratios of EGDMA:MAA. They found that the amount of niacinamide that binds to the MIP increases with the increasing initial concentration of the niacinamide between the concentrations of 0.25-5.0 mmol/L. They also estimated the binding properties of MIP further using a Scatchard equation analysis that calculates the affinity constant of a ligand to a receptor. Their results indicated that there were two distinct classes of binding sites of the MIP—a higher affinity binding site and a lower affinity binding site (Zhang and others 2005).

In addition to polymer binding characteristics, this research group also studied the performance of MIP-sensors. They attached the NAM MIP to a piezoelectric quartz crystal. They found that the degree of imprinted polymer cross-linking has no effect on the response time of the sensor, which was about 20 minutes. Lastly, Zhang and others also measured the effect of pH on rebinding of the analyte to the MIP-sensor. Though it is not clear what kind of reagent was used as the NAM carrier in the rebinding studies, it was found that the frequency shift measured by the sensor reaches its maximum at pH 7 (Zhang and others 2005).

Li and others (2005) performed a study to determine if molecular competition for binding sites affected selectivity during rebinding studies with NAM MIPs created with MAA and EGDMA. As with the researchers before them, Li and others (2005) determined that the imprinted polymer has a higher selectivity for NAM than the NIP, by more than 4-fold. It was also determined that NAM has a higher affinity than nicotinic acid with the NAM MIP (Li and others 2005).

With this information, the research group wanted to determine if there was a competition effect on selectivity when NAM and nicotinic acid together in the same solution were applied to the MIP and NIP. It was found that there is no strong competition effect with the polymer and that it was still highly selective for the template. When NAM and nicotinic acid were introduced to the polymer in a 1:1 mass ratio, the binding parameter of NAM was more than three times higher. Similar results were also obtained when the mass ratio of NAM to nicotinic acid was 1:3 (Fu and others 2001).

With the adsorption isotherms, Li and others (2005) were also able to determine using a Scatchard plot that there were two kinds of adsorption sites on the MIP to bind the NAM template, similar to Zhang and others (2005). They found that all MIPs have a high affinity binding sites, and a small amount of low affinity, non-specific binding, which is supported by previous research and stated to be inherent to non-covalent MIP synthesis (Kirsch and Whitcombe 2005; Yilmaz and others 2005; Zhang and others 2005). A notable difference in this research compared to those mentioned previously was that acetonitrile was chosen as the porogen (Li and others 2005), when it has been found that a less polar porogen favors template and monomer interaction (Wu and others 2005).

Mookda and others (2008) also conducted a study to determine selectivity of a NAM-imprinted polymer to structurally related compounds. The polymers used consisted of MAA as the functional monomer, either EGDMA or TRIM (trimethylpropane trimethacrylate) in different quantities as the cross-linker, and dichloromethane as the porogen. The primary focus of their research was to analyze binding performance in organic and aqueous media, using acetonitrile and phosphate buffer at pH 7, respectively. They also investigated the effects of using different monomers and cross-linkers on the

binding efficiency. And finally, they used a scanning electron microscope (SEM) to characterize the morphology of the optimal NAM-binding polymer (Mookda and others 2008).

Mookda and others (2008) were able to confirm previous studies stating that less polar solvents are ideal for the rebinding of the analyte to the MIP. Using acetonitrile as the rebinding solvent is more conducive to hydrogen bonding between the analyte and the MIP. When an aqueous media is used, such as the phosphate buffer at pH 7, ionic and hydrophobic interactions between the analyte, solvent and template are more dominant. And as such, there is less binding over all of the analyte to the MIP. This was tested on all of the different types of polymers made (see Table 2) using 0.25 mmol of NAM as the template (Mookda and others 2008).

Table 2. Compositions of NAM-imprinted polymers and their corresponding NIP (Mookda and others 2008)

MIP/NIP[1]	Amount Used (mmol)	
	Monomer	Cross-linker
1	Acrylamide (1.0)	EGDMA (5.0)
2	2-hydroxyethyl acrylate (1.0)	EGDMA (5.0)
3	Itaconic acid (1.0)	EGDMA (5.0)
4	MAA (1.0)	EGDMA (5.0)
5	MAA (1.0)	Divinylbenzene (5.0)
6	MAA (1.0)	Poly(ethylene glycol) diacrylate (5.0)
7	MAA (1.0)	Trimethylpropane trimethacrylate (5.0)
8	MAA (1.0)	Trimethylpropane trimethacrylate (2.5)
9	MAA (1.0)	Trimethylpropane trimethacrylate (1.0)
10	MAA (1.0)	Trimethylpropane trimethacrylate (0.5)

[1] Porogen used was 1.5ml of chloroform for all samples

Another focus of this study was the effect of different cross-linkers for NAM imprinted polymers. Between the different types of polymers made (Table 2), it was found that MIP 4 showed the highest affinity toward NAM, followed by 5, 7, and 6, respectively, suggesting that a highly flexible cross-linker such as poly(ethylene glycol) diacrylate (PEGDA) can weaken the template recognition property of MIPs (Mookda and others 2008).

Selectivity studies in this research were conducted using structurally related compounds to NAM, such as benzamide, pyridine, benzylamide, and acetophenone. When the study was conducted in acetonitrile, MIP 4 showed the best selectivity of all of

the MIPs subjected to this experiment (MIPs 4, 7, 8, 9, and 10). In aqueous buffer, only pyridine was bound to all the MIP to a lesser extent than NAM, while all of the other compounds bound more strongly to the MIP than NAM. This indicates that aqueous media is not suitable for analyte rebinding because of the aforementioned hydrophobic interactions playing a role in binding (Mookda and others 2008).

Del Sole and others (2009) also found that the nature of the solvent was important for NAM MIP synthesis. They polymerized MAA and EGDMA with NAM as a template, using acetonitrile and chloroform as two different porogens. It was found that the yields of the polymer made in acetonitrile were very low when made with the same amounts of monomers, polymerization times, and temperature as with the polymer in chloroform. They went on to further investigate the polymer made with acetonitrile and determined that if it is polymerized at a higher temperature (70°C instead of 60°C used with chloroform), the yield was increased by 43%. The reaction time was also increased and no significant difference was found. Therefore, it was concluded that temperature, not the reaction time, is significant for polymerization, in addition to the porogen (Del Sole and others 2009).

Acetonitrile solvent molecules also have hydrogen bond acceptor capacity. It was thus theorized and shown that acetonitrile molecules could form hydrogen bonds to the amidic protons if it is used as a porogen during polymerization. This interaction with the solvent blocks the amidic proton in NAM from binding to MAA. Therefore the framework of hydrogen bonds between the MAA molecules could not be established in acetonitrile (Del Sole and others 2009).

Lastly, in this research, binding capacity was evaluated, as well as selectivity. It was found that rebinding in acetonitrile was weaker than with chloroform due to the ability of acetonitrile to form hydrogen bonds with NAM. Selectivity studies were conducted using isoNAM, picolinamide, and nicotine. The polymer selectivity was shown to be similar to the results obtained by Fu and others (2001), where the isoNAM showed a significant affinity to the NAM MIP, even though it was lower than NAM, and picolinamide showed negligible affinity toward the polymer due to intramolecular hydrogen bond interactions. Nicotine also showed negligible affinity to the NAM MIP because it was a different structure altogether (Del Sole and others 2009).

Further studies were conducted by the Del Sole research group with NAM MIPs and their characteristics (Del Sole and others 2010; Del Sole and others 2011). Different ratios of functional monomer to cross-linker (MAA:EGDMA) were studied for NAM recognition capability to determine differences between highly cross-linked polymers (1:10) and low cross-linked polymers (1:1.25) (Del Sole and others 2010). It was found that a highly cross-linked polymer led to a poor binding capacity because the structure has less accessible carboxyl groups, which means interactions between NAM and carboxylic groups cannot occur. A reduced MAA:EGDMA ratio increased the overall amount of binding as the NAM binding sites are more easily accessible. However, it was mostly non-specific binding as the MIP and NIP bound nearly the same amount. The best ratio found for specific NAM to MIP interactions was 1:4 (Del Sole and others 2010).

An FTIR study was also conducted to determine the structural characteristics of the polymer. There is a peak at 1725 cm^{-1}, indicating a shift of the C=O stretching band

from 1694 cm^{-1} to 1725 cm^{-1}, as well as a disappearance of a peak at 1633 cm^{-1} that indicates the deconjugation of the C=C stretch in the MAA molecule, showing that it is polymerized (Del Sole and others 2010).

More recently, Del Sole and others (2011) determined the feasibility of using their NAM MIP in a solid-phase extraction (SPE) application to analyze a food sample. Specifically, they analyzed NAM recovery from spiked pork liver samples and compared it to the SPE of a NIP loaded cartridge, as well as the commonly used C-18 SPE cartridge. The MIP and NIP were made in a similar manner to their previous method. They found that the MIP retained 244 μg of NAM per 100 mg of the imprinted polymer and that when eluting NAM from the MIP, there was greater than 80% recovery (Del Sole and others 2011). It was also found that the NIP has a low binding capacity (Del Sole and others 2011), which agrees with what was found in previous research (Fu and others 2001; Wu and others 2003; Wu and Li 2004; Li and others 2005; Wu and others 2005; Zhang and others 2005; Mookda and others 2008; Del Sole and others 2009; Del Sole and others 2010).

The NAM standard analysis was also conducted with reverse-phase C-18 SPE cartridges as a control, since this is a typical method for neutral polar compounds. It was found that the performance is similar to the MIP SPE system. However, when a pork liver sample was analyzed on the C-18 cartridge, there was a loss of efficiency due to the complexities of the sample matrix, as there was only a 14% recovery (Del Sole and others 2011). The MIP SPE system gave an 87% recovery of NAM in the spiked pork sample. The eluted samples were analyzed with HPLC and the chromatogram showed fewer peaks with the MIP elution indicating a cleaner sample (Del Sole and others 2011).

It was also determined that there was no loss in performance of the MIP as several samples were analyzed with one polymer SPE system showing similar results each time (Del Sole and others 2011). With this in mind, MIP SPE systems should be investigated to use as a cheaper, easier, more efficient alternative to HPLC analysis for NAM.

3.5. Fourier Transform Infrared: Polymer Analysis and Identification

Infrared (IR) spectroscopy is an analytical technique based on the vibrations of the atoms of a molecule (Stuart 2004). Fourier transform infrared spectroscopy (FTIR) applies mathematical concepts developed by J. B. J. Fourier to IR spectroscopy. When Fourier concepts are applied to various terms of spectroscopy, the resultant technology creates a spectrometer that gives the entire spectrum in the amount of time that a conventional spectrometer would need to scan across just a single line in the spectrum. An FT-IR spectrometer has an interferometer rather than the grating or prism used in the conventional spectrometers, which has an infrared light source connected to it that has a beam splitter and mirrors. The interferogram obtained is a record of the signal (intensity) by the infrared detector as a function of the difference in the path for the two beams of the interferometer (Jaggi and Vij 2006).

An infrared spectrum is obtained by passing infrared radiation through a sample and determining how much of the incident radiation is absorbed at each wavelength. A peak in an absorption spectrum at a given energy corresponds to the frequency of a vibration of a part of a molecule. When a molecule is composed of different types of atoms, the vibrations are characteristic of the bonds present in the spatial arrangement. Vibrations can involve either a change in bond length between two atoms in a molecule, called “stretching,” or bond angle, called “bending.” Stretching can be symmetric or

asymmetric, depending whether the molecule bonds are stretching in phase or out phase. Bending can also contribute to infrared spectra (Stuart 2004).

For a vibrational mode of a molecule to show absorption in an infrared spectrum, it must cause a change in the dipole moment of the molecule. The larger the change, the more intense the absorption band will be. For example, in a carbonyl group, there is an inherent difference in electronegativity between the carbon and oxygen, causing it to be permanently polarized. Stretching of the carbonyl bond increases the dipole moment, resulting in an intense absorption in FTIR spectra. Symmetrical molecules have fewer "infrared-active" vibrations than asymmetrical ones because the vibrations are generally weaker and don't cause a significant change in dipole moment. Stretching of bonds between atoms from elements widely separated in the periodic table will usually give intense bands on an absorption spectrum. On the other hand, vibrations of bonds such as C—C or N=N will give weaker bands. As a molecule can contain several atoms, there will be many different vibrations occurring. The infrared spectrum can be quite complex, due to the coupling of vibrations over a large part of or the complete molecule. These are called skeletal vibrations, which can give a unique pattern, or fingerprint, of the molecule (Stuart 2004).

Infrared spectroscopy can be used to identify the composition of polymers, monitor polymerization processes, characterize polymer structure, examine polymer surfaces, and investigate processes of polymer degradation. For the scope of this review, only polymer composition and structure characterization will be discussed. As each molecule has a unique pattern on an infrared spectrum, the same follows for a polymer. Infrared spectroscopy can be used to identify polymer mixtures and whether two

polymers are miscible with each other. If they are immiscible the two polymers' spectrum should be the sum of the individual polymers' spectra. On the other hand, polymers that are miscible may have undergone some chemical interactions, leading to differences between the individual polymers' spectra and the blend's spectrum. In general, wavenumber shifts and band broadening are considered indicative of chemical interactions within a blend (Stuart 2004). This would be similar for spectra of monomers that are polymerized.

Copolymers of two different polymers can also be quantified by creating a standard curve of known compositions based on the ratio of two characteristic peaks of the two polymers. Once a standard curve is created, a mixture of the two polymers in unknown quantities can be determined by inputting the ratio of the two characteristic peaks of the spectra into the equation derived from the standard curve (Stuart 2004).

FTIR can also be utilized for determining polymeric structure. If a polymer is composed of multiple types of monomers, characteristic bonds can assist in determining the structure of the polymer based on band shifts from monomer to polymer. For example, in a MIP created with MAA and EGDMA and niacinamide as template, a peak at 1725 cm^{-1} showed that there was a shift of the C=O stretching band from 1694 cm^{-1} to 1725 cm^{-1}, which indicated there was a loss of conjugation of the carboxylic acid group during polymerization (Del Sole and others 2010). For this reason, FTIR is a common tool used for characterization of MIPs.

3.6. Microfluidic Chips

Microfluidic chips are often called "lab on a chip" or micro-total analytical systems. This is because the intentions for these devices are to be able to conduct an

analysis from start to finish in a portable microsystem. Normally they are made of a polymer such as PMMA or polydimethyl siloxane (PDMS), but can also be made of glass or silicon. A miniscule amount of sample, as low as 0.5 µl, is injected into a sample reservoir. The sample flows through the column, typically with electroosmotic flow, separating analytes by charge, but can also be with pressure flow, separating analytes based on laminar flow properties (Lutz and others 2003). The most basic design of a microfluidic chip channel is that of a simple cross injection design as shown in Figure 3. The sample is typically introduced through the sample reservoir, but may also be introduced on either of the two side ports. The two side ports can also be used to introduce other reagents or buffers aiding in a reaction or flow through in the microfluidic channel.

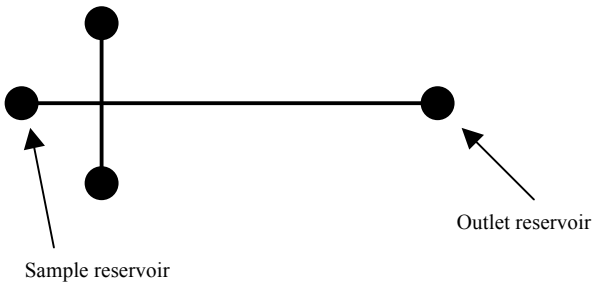

Figure 3. Schematics of a simple cross injection design of microfluidic chips.

Each analyte is detected at the end of the channel by some type of detection method, such as laser-induced fluorescence or an electrochemical detection method (Atalay and others 2011).

Microfluidic chips are increasingly being researched for nano-scale analyte separation protocols or chromatography-type applications. The majority of the published works in the study of microchip analysis pertains to CE-type applications, while the chip-

based liquid chromatography (LC) development has been slower. A summary of the pros and cons of LC and CE can be found in Table 3. Because LC is quite versatile and efficient, its miniaturization is particularly attractive because the experimental conditions can be adapted for analyzing various samples with varying analyte compositions and polarities (Harris 2003). On the other hand, CE has a few drawbacks, such as sampling bias under applied electric fields, exposing samples to high voltage, and Joule heating effects (Fuentes 2007). As mentioned in Table 3, LC has drawbacks with the use of high pressure pumps and large organic solvent volumes. The development of a chip-based miniaturized chromatography would have an immense impact on separation science, as these disadvantages would be very reduced or eliminated (Harris 2003).

Table 3. Comparison of advantages and disadvantages of LC and CE (Serwe 2000; Aurora Prado and others 2005; Fuentes 2007)

Liquid Chromatography	Capillary Electrophoresis
Pros:	Pros:
• Many different types of detection methods	• Simpler instrumentation
• Good reproducibility	• Higher analyte separation efficiency
• Many different types of stationary phases	• Low consumption of solvent
• Well-established methods	
Cons:	Cons:
• Uses high pressure pumps	• Uses high voltage electricity
• Large organic solvent volumes	• Cannot use samples with high or low pH

The need to miniaturize other device components to minimize the dead volume contribution is one of the major challenges limiting the development of miniaturized LC systems. Microfabrication has the potential to allow monolithic integration of several components in a single substrate. However, most microfabricated LC devices that have been reported have only miniaturized the separation channel while continuing to maintain an external pump mechanism such as a syringe pump (Sato and others 2003; Fuentes 2007), or are connected to external pressurized gas cylinders or vacuum systems (Grover and others 2003). Therefore, according to Fuentes and others (2007), the development of pumping systems that are capable of applying pressure to generate appropriate nL-

μL/minute flow rates required for microfabricated channels is critical to the success of microfluidic chip-based LC (Fuentes 2007).

Another key challenge in the development of chip-based LC is the introduction of stationary phases into channels. Columns packed with porous materials may be the most prevalent separation media for LC. However, introducing small diameter microparticles at desired locations within microchannels is not easy (Oleschuk and others 2000; Slentz and others 2001; Jemere and others 2003). The main drawback to preparing packed beds on a microfluidic channel is the necessity to construct and position a retaining frit at the end of the channel to keep the particles in, but allow flow-through of reagents (Fuentes 2007). Recently, the use of monoliths for chromatographic separations has been studied. A monolith is composed of a continuous piece of solid material with interconnected pores, and can be created via in-situ polymerization of monomers in a microfluidic channel, which avoids the tedious step of packing the channel with microparticles (Fuentes 2007). In a design by Slentz and others (2001), strictly defined and distributed particles are fabricated directly in the microfluidic channel of the chip. This method is based on the development of collocated monolithic support structures (COMOSS) etched in quartz crystal previously described (He and others 1998). COMOSS are tiny microstructures cast from a single material created side by side within the column. However, instead of quartz, the COMOSS were molded in PDMS.

The dimensions of the monolithic structures were 10 x 10 μm, separated by 5 μm channels. The results of this study indicated that COMOSS separation columns within microfluidic chip channels can serve as an inexpensive, low-volume, separation technique (Slentz and others 2001). COMOSS is advantageous over packing a channel

with microparticles as the monolith can be bound covalently to the channel surface, as well as be confined to illuminated areas of the channel if the polymerization of the COMOSS is light-initiated. Thus, detection windows and injection arms can be defined by selective casting of the polymer (Stachowiak and others 2003). More importantly, the high porosity and mass transfer that can be achieved in COMOSS applications should prevent the need for high-pressure pumping systems that may be otherwise needed for applications in microfluidic chip-based LC (Fuentes 2007).

3.5.1. Microchip Methods for Food

Using microchips for food analysis is a relatively recent development. They have the possibility to be quite useful in the food environment because they are inexpensive, portable, require minimal use of sample and reagent, and can potentially be used on-site by anyone rather than specialized, trained personnel (Escarpa and others 2007). One of the first applications of microchip capillary electrophoresis for food analysis was for phenolic acids, such as chlorogenic, gentisic, ferulic, and vanillic acids. Scampicchio and others (2004) applied this method using a glass microchip for the analysis of commercial red wine utilizing minimal sample preparation (Scampicchio and others 2004). Once the microchip method was optimized, it was determined that this method was suitable for low levels of phenolic acids in commercial red wine. Scampicchio and others (2004) also explored different oxidation potentials to improve selectivity and obtain clearer electropherograms. They determined that lower potentials gave greater selectivity and higher potentials provided greater sensitivity (Scampicchio and others 2004). The dilution performed on the wine samples assisted in circumventing interference of other phenolics, such as flavonoids (Escarpa and others 2007). Sample preparation is an important consideration for food analysis, especially for microfluidic chips.

Blasco and others (2005) optimized the conditions of CE microchips with electrochemical detection for the analysis of prominent natural antioxidants in food environments (Blasco and others 2005). The simultaneous separations of flavonoids and vitamins were shown for the first time. It was proposed to electrophoretically separate the antioxidants as "analyte couples" to help with the interpretation of the electropherogram. The analyte couples were chosen based on their presence or absence to show positive or negative identification proof, respectively, in pear pulp and juice samples. The separations of the couple analytes were categorized as such: two prominent phenolic and non-phenolic antioxidants, (+)-catechin and ascorbic acid, respectively; two prominent flavonoids that are characteristic to the peripheral parts of the pear fruit such as the peel, (+)-catechin and rutin; and two fingerprint phenolics arbutin and phlorizdin, which are typical of pears and apples, respectively. Once the analytical method was optimized, it was applied to fresh pear pulp and pear juice samples. Solid samples were extracted with methanol and centrifuged prior to analysis in the chips. Juice samples were also centrifuged, and then filtered before analysis (Blasco and others 2005).

The results showed that all three analyte couples could be detected in a pear pulp and juice matrix when spiked and only arbutin, (+)-catechin, and ascorbic acid were detected, as expected in juice. Rutin was not expected to be detected since it is found in the peels of the fruits, which were to be removed prior to processing; phlorizdin was not detected in the juice, indicating that there was no adulteration with apple juice. Blasco and others (2005) proposed that dilution and pH and ionic strength conditions may be important for the analysis of food samples, as they noticed the migration times of ascorbic acid decreased with the spiking of analytes into the sample matrix (Blasco and

others 2005). Though the pear matrix was complex and only detected prominent phenolics (Blasco and others 2005), this research provided insight into the application of microfluidics chips in the food environment, specifically for quality control purposes.

Crevillén and others (2006) determined the content of water-soluble vitamins in a supplement form using microchip CE with electrochemical detection (Crevillén and others 2006). The same type of simple cross injection microfluidic chip was used as mentioned above in the previous studies by this group (Blasco and others 2005; Crevillén and others 2006). Optimal conditions were determined and separation of a sample containing standards of pyridoxine, ascorbic acid, and folic acid was achieved in less than 130 seconds. It was also shown that, compared to results with separation buffer in the detection reservoir, the presence of nitric acid in the detection led to sharper peaks, greater sensitivity, and less baseline noise, as well as noticeably improved the performance of detection of folic acid since it became a neutral compound from the protonation and was no longer repelled from the surface of the electrode (Crevillén and others 2006).

After optimization of the method, commercial nutraceutical formulations for these vitamins were analyzed to demonstrate its capabilities. The results were within good precision and repeatability, and the amounts of vitamin determined by the microchip protocol matched closely to the amount declared by the manufacturer, with the relative error range between 2-9%. Samples with higher mineral salt content were more difficult to analyze due to problems of the intrinsic features of electrokinetic injection, such as modification of ionic strength and compatibility between buffers, solvents, or matrices, (Crevillén and others 2006).

3.7. Use of Molecularly Imprinted Polymers with Microfluidic Chips

To date, the use of MIP technology with microfluidic chips has not been widely explored. The majority of the research involving MIP with microfluidic chip technology pertains to the detection of the analyte, rather than separation.

Huang and others (2006) first integrated a microfluidic system with MIP films that were created for surface plasmon resonance (SPR). A thin film MIP was created for the detection of progesterone and then, for cholesterol and testosterone to demonstrate the flexibility of this method. The MIP films were spin-coated inside separate reaction chambers of the same microfluidic system, which enabled sensing of multiple biomolecules via SPR. Micropumps and microvalves were integrated into the chip to control the sample introduction process to determine the number of molecules adsorbed to the MIP films. With this apparatus, cholesterol, and testosterone were successfully determined at normal concentrations found in the human body, whereas progesterone needed a concentration step associated with it as it is found in lower concentrations (Huang and others 2006).

Hong and others (2010) were one of the more recent groups to investigate this combination by creating a disposable microfluidic biochip with on-chip MIP biosensors to optically detect propofol, an anaesthetic. The MIP was fabricated as a membrane, and was placed in a microfluidic chamber on the plastic microfluidic chip, which was fabricated with the channels and then bonded to a solid layer. With this method, the successful detection of the concentration of propofol was attained within 60 seconds. The measurements at different concentrations show a linear relationship between 0.25 ppm and 10 ppm, indicating a high level of sensitivity (Hong and others 2010).

Chapter 4. Materials and Methods

4.1. Chemicals

All chemicals were purchased from Sigma Aldrich Chemical Co. or Fisher Scientific unless otherwise specified. AIBN was purchased from MP Biomedicals LLC. Chloroform was dried by storing it over type 4A, 8-12 mesh molecular sieve beads, made of sodium alumino-silicate purchased from BDH Chemicals.

4.2. Polymer Synthesis and Preparation

4.2.1. Melamine-co-Chloranil Polymer with L-Ascorbic Acid Template

The first objective of the project was to bind the MIP created based on Prasad and others (2008) to a PMMA support. The modified protocol for the MIP synthesis, and binding MIP to PMMA is described in sequence in Appendix 1. Once the protocol had been established, the next part was to optimize the binding capacity of the mel-*co*-chl polymer by assaying polymers created from various ratios of the monomers. The second objective was to determine optimal design of the microfluidic chip. The results of this work will be shown in the appendix, as it was discontinued once it was shown that the attachment of the polymer to a PMMA support was not successful in our lab. After this point, the overall objective of the project changed to what is now reflected in this report.

4.2.2. MAA, EGDMA, and Niacinamide Polymer with Benzoyl Peroxide

The protocol used by Mookda and others (2008) was followed as described in the article. The method is summarized in Figure 4. The polymer created was one reported to have a better binding capacity and specificity and it used MAA as the monomer, EGDMA as the cross-linker and dichloromethane (DCM) as the porogen. This reaction

also used benzoyl peroxide as the free radical initiator (Mookda and others 2008). However, when the polymerization reaction was left for 24 hours at 60ºC as described in the publication, it became very glass-like and difficult to extract for analysis. The polymer was made with 5 ml of porogen instead of 1.5 mL because when 1.5 mL DCM was

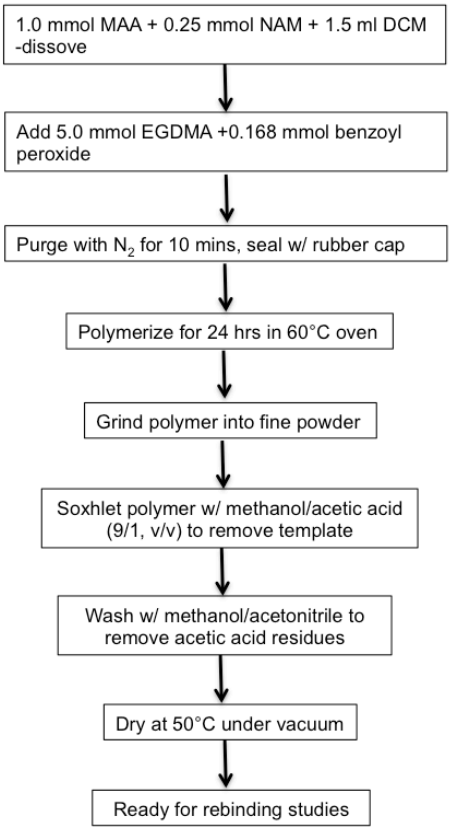

Figure 4. Method for MIP synthesis by Mookda and others (2008). NIP created by omitting NAM template

used, the solvent evaporated in the test tube, even when sealed in the best way possible. The resulting polymer was still very hard, glassy, and difficult to remove. Another polymer was created using this method but with a shorter polymerization time and using more solvent.

A 7/3, v/v methanol/acetic acid instead of 9/1 v/v, reported by Mookda and others (2008) was used during the soxhlet for better extraction of the template. The shortcomings of this method included a minimum 24-hour soxhlet extraction of the template bound initially, as well as the difficulty of achieving the optimal degree of polymerization before the polymer turns to a glass state.

4.2.3. MAA, EGDMA, and Niacinamide Polymer with AIBN

The polymer used for all other analyses moving forward was based on the Del Sole and others (2010) method. As the ratio of monomer, cross-linker, and template varied depending on the type of experiment, only the general synthesis method will be discussed here. Details on the amounts of the components used can be found in section 4.3.

EGDMA and MAA were measured out into glass scintillation vials. For the MIP, NAM was measured out separately and then dissolved into the EGDMA and MAA solution. The NIP was prepared with the same method as the MIP, but without the addition of NAM or other template. Dry chloroform was then added into the vials, which were then placed in the Elmasonic S30H sonicator bath (Germany) for 5 minutes. After sonicating, 0.01 g of AIBN was added to the solution and the vials were sonicated again for 5 minutes. The vials were flushed again with nitrogen gas for 2 minutes and sealed. A sand bath was pre-heated on a hot plate to be above 60ºC for about 30-45 minutes in order to equilibrate to 60ºC when transferred to the incubating oven. The vials were then placed in the sand bath with sand covering over the solvent line and were allowed to polymerize in a force draft oven set at 60°C for 16 hours.

After polymerization, the vials were taken out of the oven and sonicated for 5 minutes as described in Del Sole and others (2010). Polymers were vacuum filtered in a

fumehood with a Buchner funnel and Whatman #1 filter paper. Polymers were left to air dry on a glass petri dish in the fume hood. When dry, the polymers were crushed to a fine powder in a mortar and pestle.

Polymers were rinsed 10 times with 10 mL of 8:2 100% ethanol:1M acetic acid solution in new scintillation vials and centrifuged for 5 minutes in a International Clinical Centrifuge, model CL, from International Equipment Co. (Needham Heights, Massachusetts) at the highest setting, discarding the supernatant each time. On the final rinse, the supernatant of the polymer was collected and analyzed in triplicate on a Nanodrop 1000 UV spectrophotometer (ThermoScientific, Wilmington, Delaware) at 262 nm to ensure that there was no residual NAM template. The precipitate was left to air-dry in a glass petri dish. After drying, the washed polymers were crushed with a mortar and pestle into a fine powder. The NIP was rinsed similarly to the MIP, but only 3 times.

4.3. Monomer:Cross-linker Molar Ratio and AIBN Studies

Polymers for the different ratios of MAA:EGDMA studies, as well as for the different amounts of AIBN, were made similar to the method described in section 4.2. Table 4 lists the amounts of MAA, EGDMA, NAM, AIBN used in different trials.

Table 4. Amounts of monomers, NAM solution in chloroform, and initiator added for different polymer studies.

MAA:EGDMA Ratio	MAA (mmol)	EGDMA (mmol)	NAM (mM)	AIBN (g)
1:4	1.55	6.30	43	0.01
1:4	1.55	6.30	43	0.02
1:4	1.55	6.30	43	0.03
1:0.75	1.55	1.16	233	0.03
1:1.25	1.55	1.94	140	0.03
1:2	1.55	3.10	87	0.03
1:3	1.55	4.65	58	0.03
1:5	1.55	7.75	35	0.03
1:6	1.55	9.3	29	0.03

4.4. Rebinding Studies with Niacinamide, Benzamide, Pyridine, and Acetamide

For all rebinding studies, the analyte of interest was made in a 1 mM solution using acetonitrile as the solvent. Rebinding studies were conducted using NAM, as well as benzamide, pyridine, and acetamide for polymer selectivity studies. Twenty milligrams of MIP and corresponding NIP were weighed out in triplicate in a microcentrifuge tube. A 1 ml aliquot of a 1 mM analyte solution was added to each tube. An aliquot of the analyte was saved for analysis as the "initial amount." Polymers were mixed with the solution using a vortex, and left to rotate for approximately 16 hours on a Labquake rotator (Barnstead/Thermolyne, Dubuque, Iowa) at 8 RPM.

After rotation, the tubes were centrifuged in a Mikro 20 Centrifuge (Hettich, Tuttlingen, Germany) for 10 minutes at 13,000 RPM. The supernatant was collected and clarified using a 0.45 μm pore nylon filter into a separate tube and refrigerated until ready for analysis. Supernatants with NAM and pyridine were analyzed using a Nanodrop 1000 UV Spectrophotometer at a wavelength of 262 nm and 254 nm, respectively. Benzamide was analyzed with an HP Agilent 1100 HPLC System (Waldbronn, Germany) with a quaternary pump system and photo diode array detector using a 4.6 x 250 mm, 5 μm particle size Supelcosil LC18 column with 1 mm Optiguard C18 guard cartridge. The mobile phase contained 50 mM sodium dihydrogen phosphate adjusted to pH 3.0 with orthophosphoric acid/methanol 60:40 isocratic method, with a flow rate of 0.7 ml/minute and sample injection volume of 10 μl. Acetamide was also analyzed with the same system. The mobile phase contained a 97:3 ratio of water:methanol, with a flow rate of 1.0 ml/minute and a sample injection volume of 10 μl. Analyte quantities were determined using the difference between the "initial amount" and the amount determined from the supernatants.

4.5. Fourier Transform Infrared (FTIR) Spectroscopic Analyses

Polymer samples in a microcentrifuge tube from the rebinding studies were rinsed with 1 mL of acetonitrile to remove excess unbound NAM before analyzing with FTIR. These samples were analyzed to determine if bound NAM could be detected using FTIR. Additional, newly synthesized polymers were also analyzed once the template was removed for comparison. Polymers for FTIR were dried in a 60°C force draft oven overnight and kept in a desiccator until ready for analysis. Before analysis, polymers were loosened from the tube with a small metal spatula.

FTIR used was a Perkin Elmer Spectrum 100 with Universal Attenuated Total Reflectance (UATR) attachment (Lantrisant, United Kingdom). Prior to sample analysis, the background scan with no sample on the UATR attachment was conducted to standardize the instrument. A small amount of powdery sample was introduced onto the UATR sample reservoir, and was compacted down with the UATR arm. Samples underwent up to 50 scans with a resolution of 4 cm^{-1}.

4.6. Scanning Electron Microscope Analyses

Scanning electron microscope images were taken with a Hitachi S-4700 microscope at the University of British Columbia Bioimaging Facility. Samples were mounted onto 6 mm carbon sticky pads and were coated with a 5-6 nm gold-paladium with a Cressington sputter coater. The accelerating voltage used was 1.0 kV with a working distance of 3.0 mm.

4.7. Statistical Analysis

Replicates for each trial were conducted in triplicate using the same batch of polymer. Each trial was conducted with a different batch of polymer. ANOVA and Tukey's test was conducted using Minitab 15. Standard deviations were determined using Microsoft Excel. Coefficients of variation (CV) were calculated to determine the relative standard deviation.

Chapter 5. Results and Discussion

5.1. MAA, EGDMA, and Niacinamide Polymer with Benzoyl Peroxide

When the polymerization reaction was left for 24 hours at 60ºC as described by Mookda and others (2008), it became very glass-like and difficult to remove for analysis. After 1.5 hours of polymerization, most replicates appeared to be a translucent white, waxy solid, with some starting to turn slightly yellow, while others were still liquid. The replicates that were still liquid were left in the 60ºC incubator for further polymerization for another 1.5 hours and appeared to be yellowy-brown solids. All solid polymers after 1.5 hours and 3 hours were able to be broken up and crushed with a spatula and had a waxy texture, regardless of white or yellow colour. The yellow colour was later determined to be an oxidation reaction between the benzoyl peroxide and NAM. This was confirmed when NAM was incubated with DCM and benzoyl peroxide at 60°C overnight, and the resulting liquid was yellowy-brown instead of colourless, indicating that the initiator actually oxidized the NAM; the control incubation of DCM and NAM showed a colourless, clear liquid.

With the qualitative findings, in addition to the complexities of template removal using a soxhlet apparatus for 24 hour and inconclusive results, this method was not deemed satisfactory and another MIP using NAM as the template was investigated.

5.2. MAA, EGDMA, and Niacinamide Polymer with AIBN Rebinding Studies

The MIP used by Del Sole and others (2010) used a 1:4 ratio of monomer (MAA):cross-linker (EGDMA). During initial experiments of this method, the polymer was created in this molar ratio and rebinding studies were conducted with 1mM NAM in

acetonitrile to ensure specific binding. Rebinding studies were conducted on three separate occasions and it was determined that NAM binding did occur specifically to the MIP, and less so with the NIP. An imprinting factor was determined using the equations from Mookda and others (2008). The amount of NAM bound to the polymer

$$Q = Q_{initial} - Q_{unbound} \quad (1)$$

was determined from the initial amount of NAM, $Q_{initial}$, before adding it to the polymer and the amount of NAM that did not bind to the polymer, $Q_{unbound}$. The amount bound to the polymer, Q, is used to determine the percentage bound

$$\%Bound = Q/Q_{initial} \, x \, 100 \quad (2)$$

Then the imprinting factor

$$IF = \%Bound_{MIP} / \%Bound_{NIP} \quad (3)$$

was determined as the ratio between the percentage of NAM bound to the MIP to the percentage of NAM bound to the NIP. In each rebinding study, three replicates of each polymer were used to determine the percent bound. Table 5 summarizes the imprinting factors found for each trial.

Table 5. Imprint factors[1] and binding capacity[2] for 3 trials of 1:4 MAA:EGDMA polymers compared with literature results

	Imprinting Factors[1]	Binding Capacity[2] (mg/g pol)
Trial 1	2.16 ± 0.72 (33)	2.46 ± 0.16 (7)
Trial 2	1.13 ± 0.19 (18)	1.31 ± 0.14 (10)
Trial 3	2.25 ± 0.51 (23)	1.60 ± 0.25 (16)
Del Sole (2008) 1:4 Polymer	2.3	15.3 ± 1.4

[1] Imprinting Factor = %BoundMIP/%BoundNIP (mean of 3 replicates ± std dev (CV))
[2] Binding Capacity = mg NAM bound to MIP per g polymer (mean ± std dev (CV))

A one-way analysis of variance (ANOVA) of the three trials determined that the difference between the imprinting factors were not statistically significant from each other ($p=0.071$). However, if the standard deviation of the assay were smaller, then there would likely be a significant difference.

The imprinting factors of the experimental 1:4 polymers were similar to that found by Del Sole and others (2010) for their 1:4 ratio polymer, as can be seen in Table 5. However, the binding capacity reported in the paper was significantly higher than the experimental values obtained in this work. This could be due to changes in the rebinding study procedures made from Del Sole and others' (2010) work. In their work, the rebinding procedure involved 20 mg of dry polymer with 5.0 ml of a 4 mM NAM solution in chloroform (Del Sole and others 2010), whereas in this research, 1 mM of NAM dissolved in acetonitrile was used. However, it has been shown afterward in our lab that using a higher concentration of NAM may be more beneficial for achieving a higher quantity bound to the polymer, but we were still unable to get a similar high yield in binding capacity compared to quantities reported by Del Sole and others (2010), which show a maximum binding capacity of 19.3 mg NAM bound/g polymer at 5 mM. In this present study, an MIP and NIP were also rebound with different NAM concentrations in acetonitrile. Figure 5 shows the binding capacity of both MIP and NIP against the NAM concentration. The binding capacities show a saturation where the binding capacity increases greatly initially, but eventually plateaus. The difference between the MIP and NIP binding capacity became greater as NAM concentration increased, which increases the overall imprinting factor. Therefore, as the NAM concentration increases during

rebinding, there is more NAM binding with the cavities, suggesting that it may be more beneficial to use a higher concentration of NAM when performing rebinding studies.

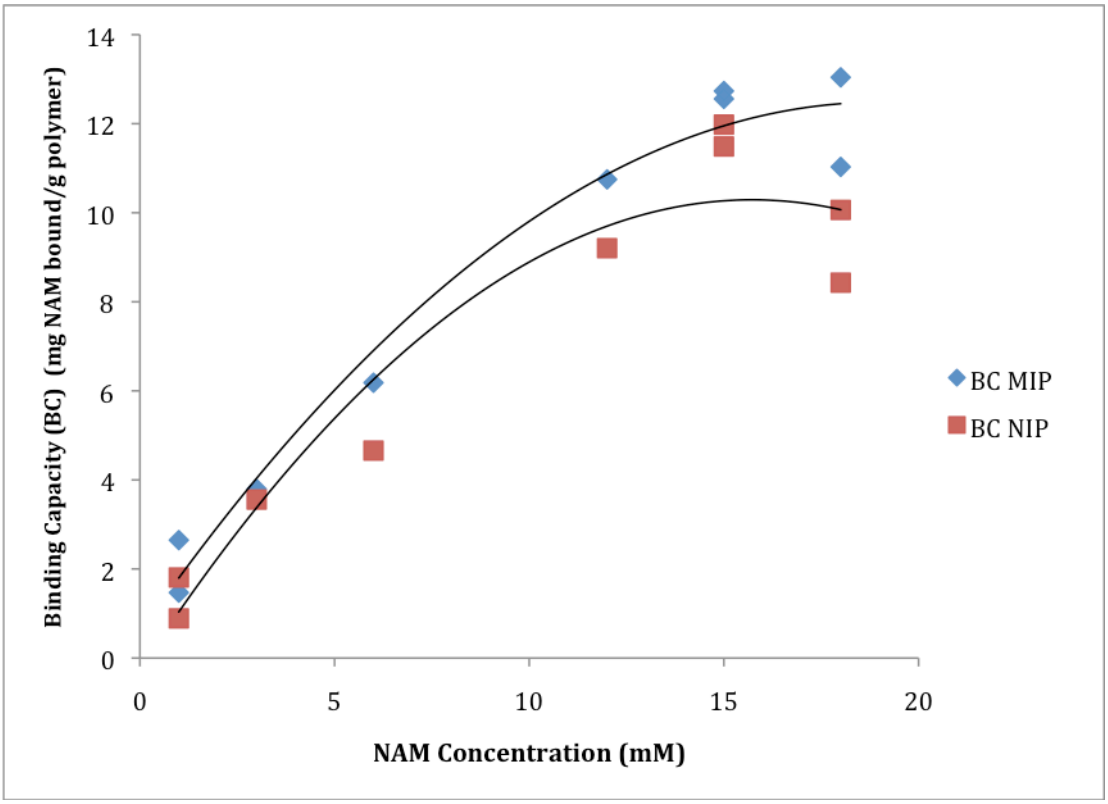

Figure 5. Binding capacity of MIP/NIP versus NAM concentration (Koo, unpublished).

It has been mentioned that less polar solvents for rebinding studies favor the interaction between the analyte and MIP (Yilmaz and others 2005; Mookda and others 2008). Acetonitrile is a common solvent used in rebinding studies (Mookda and others 2008). However, it has more polarity than chloroform. It was found that the NAM and MAA interaction is weaker in an acetonitrile medium. It has also been concluded that conducting rebinding studies using acetonitrile as the solvent is not as effective because NAM and acetonitrile interact with each other, thus competing with MAA for its hydrogen bonding sites (Del Sole and others 2009). Even with this knowledge,

chloroform was not used in rebinding studies for this present research, as it was difficult to dissolve enough NAM to make a 1 mM solution. Finally, chloroform is not suitable for the polypropylene syringe filters that were reported to be used by Del Sole and others (2010) (Cole Parmer Canada Inc. 2011). Therefore, the results from Del Sole and others (2010) could not be reproduced.

5.3. Differing Amounts of AIBN Used

MIP formation was inconsistent using 0.1 g of AIBN, as sometimes a polymer would form completely, and other times it would just turn into a cloudy liquid, which may be due to partial polymerization of the monomers. It was found that the addition of more AIBN led to more complete polymerization reactions. However, it wasn't clear if the amount of AIBN affected the final results and imprinting factor. Recommended appropriate amounts of initiators to use were not stated in many previous works (Mookda and others 2008; Del Sole and others 2010). Additionally, a previous paper by Del Sole and others state using 0.15 mmol of AIBN for a batch size of 40 mL, which equates to approximately 25 mg (Del Sole and others 2007). On the other hand, another researcher used 40 mg for a 10 mL batch size (Fu and others 2001). With the inconsistency in AIBN usage, it was important to know whether it played a role in differing MIP formation processes and thereby if it affected the analyte rebinding to the polymer.

An experiment was conducted by creating a series of 1:4 MAA:EGDMA polymers using 0.01, 0.02, and 0.03 g of AIBN. The results are summarized in Table 6. A one-way ANOVA showed that the results were not statistically different ($p=0.089$). Subsequently, 0.03 g of AIBN was used as a standard amount in all reactions to ensure full polymerization.

Table 6. Imprinting factor of 1:4 (MAA:EGDMA) polymers using varying amounts of AIBN

AIBN (g)	Imprinting Factor[1]
0.01	2.25 ± 0.51 (23)
0.02	1.70 ± 0.18 (11)
0.03	2.37 ± 0.10 (4)

[1] Imprinting Factor = %BoundMIP/%BoundNIP (Mean of 3 replicates ± std. dev.(% CV))

5.4. Ratios of MAA to EGDMA

It was imperative to determine the optimum ratio of monomer to cross-linker to find out whether the 1:4 ratio we were using was ideal. It was previously mentioned that a ratio of 1:3 had the best rebinding performance (Del Sole and others 2010), while in another study a 1:5 ratio is used throughout (Mookda and others 2008). In my studies, polymers were created with a range of different ratios of MAA:EGDMA including 1:0.75, 1:1.25, 1:2, 1:3, 1:4, 1:5, and 1:6. These were chosen based on the different ratios studied by Del Sole and other (2010), such as 1:1.25, 1:3, and 1:4, as well as for testing additional ratios. Imprinting factors were determined from rebinding studies from all polymers and are summarized in Table 7. The 1:4 MAA:EGDMA polymer had a statistically higher imprinting factor from all others, which were similar to each other.

Table 7. Imprinting factors from the polymers formed using different ratios of MAA:EGDMA

Polymer MAA:EGDMA Ratio	Imprinting factor[1]
1:0.75	0.89 ± 0.011^{a} (1)
1:1.25	1.49 ± 0.069^{a} (5)
1:2	1.29 ± 0.064^{a} (5)
1:3	1.42 ± 0.16^{a} (11)
1:4	2.25 ± 0.51^{b} (23)
1:5	1.35 ± 0.21^{a} (15)
1:6	1.47 ± 0.16^{a} (11)

[1] Imprinting Factor = %BoundMIP/%BoundNIP (Mean of 3 replicates ± std. dev.(% CV))

In addition to the imprinting factor, it was interesting to see the characteristics of the rebinding study on each polymer. Table 8 shows the mean percent NAM bound to each MIP and NIP. Out of all the % bound in the MIP, the 1:3 and 1:4 MAA:EGDMA ratio polymers were not significantly different from each other, and the 1:4, 1:5, and 1:5 ratio polymers were not significantly different from each other.

Table 8. Percent NAM bound to both MIP and NIP of the polymers of different MAA:EGDMA ratios

Polymer MAA:EGDMA Ratio	% Bound on MIP[1]	% Bound on NIP[1]
1:0.75	52.5 ± 0.68[a] (1)	58.9 ± 0.96 (2)
1:1.25	63.5 ± 2.95[b] (5)	42.6 ± 0.71 (2)
1:2	35.6 ± 1.77[c] (5)	27.54 ± 2.20 (8)
1:3	23.96 ± 2.64[d] (11)	16.87 ± 1.24 (7)
1:4	20.39 ± 4.65[de] (23)	9.07 ± 2.63 (29)
1:5	16.17 ± 2.46[e] (15)	11.95 ± 1.49 (13)
1:6	13.38 ± 1.45[e] (11)	9.08 ± 0.36 (4)

[1] Mean of 3 replicates ± std dev (cv)

For the 1:0.75 MAA:EGDMA polymer, more NAM bound to the NIP rather than the MIP, which is why there is a low imprint factor. This could be because during polymer formation, the NAM template tied up some of the hydrogen bonding sites. It is also possible that there may not have been complete removal of the template, as some might have been covalently bound within the polymer. However, as MAA is the functional monomer, it is logical that there is overall more binding of NAM to the polymer than in the 1:4. But it is evident that this binding is non-selective.

As the ratio of MAA:EGDMA decreases, Table 8 shows that the overall percentage of NAM bound decreases as well. Just as with the 1:0.75 MAA:EGDMA polymer, in the 1:6 MAA:EGDMA polymer there is less specific binding occurring. This may be because in a highly cross-linked polymer, there could be more exposure of the

functional monomer, while simultaneously having fewer binding sites and the template doesn't seem to have a great effect in inducing selectivity on the MIP. The imprint factor for the 1:4 MAA:EGDMA polymer is the greatest (Table 7). Therefore, it was logical to continue to use this ratio for further MIP studies involving NAM as a template.

Mookda and others (2008) showed that the ratio of monomer to cross-linker plays a key role for MIP specificity and affinity. They showed that an MIP with a 1:1 MAA:trimethylpropane trimethacrylate (TRIM) ratio, had the highest affinity toward NAM with a high relative specificity when compared with the rebinding studies of structurally similar compounds to NAM. This indicated that the ratio of monomer to cross-linker should be optimized, as the other ratios of MAA:TRIM didn't have such promising values (Mookda and others 2008).

Zhang and others (2005) studied the influence of different ratios of cross-linker to functional monomer using NAM as the template, EGDMA as the cross-linker, and MAA as the template. They determined this influence on the performance of MIP-modified piezoelectric sensors. The theory is that sensors with MIPs bound to them have a higher affinity for a specific analyte that is used as the MIP template - in this case, NAM. In their research, they determined that the EGDMA:MAA ratio dictates the uniformity of the particle size. For example, they found that when the ratio was less than 3:1 or over 20:1, the size of the polymer particles was non-homogeneous. However, when the ratio was between 3:1 and 20:1, they were able to obtain homogeneous polymer particles sized around 0.1 μm (Zhang and others 2005). In the presented research, microparticles were not obtained, but rather the polymerization led to a non-homogeneous agglomerate. It is possible that Zhang and others (2005) and Del Sole and others (2010) obtained

microspheres because the polymerization was conducted in a larger volume and the glassware or apparatus used was more conducive to forming particles, such as the use of a round bottom flask and a rocking table during incubation. Additionally, a larger volume of porogen may increase the chance of obtaining microspheres because the porogen creates more pores and the polymer is less likely to self-aggregate. According to Ye and Mosbach (2001), the excess porogen dissects the MIP microgel forming them into microspheres while keeping the specific imprinted sites intact. The porogen should be in excess by 95% or more compared to the prepolymerization mixture (Ye and Mosbach 2001). In this study, the polymerization was conducted in 20 mL glass scintillation vials for economic reasons and practicality for the sand bath.

Their results indicated that there were two distinct classes of binding sites of the MIP—a higher affinity binding site and a lower affinity binding site (Zhang and others 2005). They further went on to explain that the apparent number of all affinity binding sites, high and low, and dissociation constant increase with increasing amount of cross-linking (higher ratio of EGDMA:MAA), but when the ratio is over 20:1, they decrease. This may be due to the fact that the polymer particle sizes are inhomogeneous (Zhang and others 2005).

In addition to polymer binding characteristics, this research group also studied the performance of MIP-sensors. They attached the NAM MIP to a piezoelectric quartz crystal. They found that the degree of imprinted polymer cross-linking has no effect on the response time of the sensor, which was about 20 minutes. They did, however, show that the selectivity of the sensor increases with the degree of polymer cross-linking up to a ratio of 20:1 and higher. The stability of the MIP-modified sensor was quite good for

ratios of cross-linker to MAA over 3:1, as they were able to use the same sensors for multiple tests. Ratios below 3:1 are less stable, which may be due to the necessity of having enough cross-linker to link the polymer complex completely. The degree of cross-linking has influence on a MIP's properties such as rigidity of the cavity and flexibility of the polymer.

Further studies were conducted by the Del Sole research group with NAM MIPs and their characteristics (Del Sole and others 2010; Del Sole and others 2011). Different ratios of functional monomer to cross-linker (MAA:EGDMA) were studied for NAM recognition capability to determine differences between highly cross-linked polymers (1:10) and low cross-linked polymers (1:1.25) (Del Sole and others 2010). It was found that a highly cross-linked polymer led to a poor binding capacity because the structure has less accessible carboxyl groups, which means interactions between NAM and carboxylic groups cannot occur. A reduced MAA:EGDMA ratio increased the overall amount of binding as the NAM binding sites are more easily accessible. However, it was mostly non-specific binding as the MIP and NIP bound nearly the same amount. The best ratio for specific NAM to MIP interactions was 1:4 (Del Sole and others 2010).

5.5. Rebinding Studies of Structurally Related Compounds compared to Niacinamide

To determine which functional groups of NAM the MIP had affinity for, rebinding studies were conducted using chemicals that contained a single functional group of the NAM molecule. Experiments evaluating the binding of 1 mM solutions of acetamide and benzamide, and 2 mM solution of pyridine in acetonitrile were conducted. As shown in Figure 6, acetamide represents the NAM molecule without the pyridyl group

attached; pyridine represents the NAM molecule lacking the acetamide function; and benzamide is similar to NAM, but does not contain a pyridyl nitrogen. Neither benzamide nor acetamide exhibited an absorbance peak that could be used for quantitation. With UV spectrophotometric analysis, only pyridine and NAM rebinding could be determined because there may have been interference with acetamide and benzamide in the analyte elution solution and the quantity of unbound acetamide and benzamide could not be resolved. In both acetamide and benzamide rebinding, the the absorbance after the rebinding ($Q_{unbound}$) was higher than the absorbance for $Q_{initial}$, giving a "negative binding."

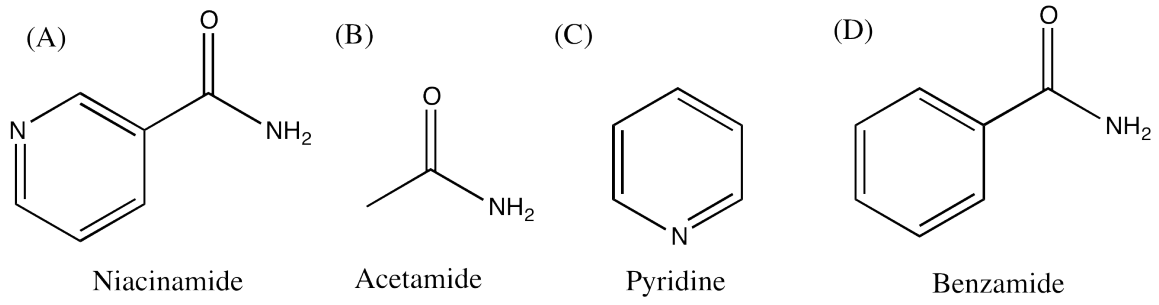

Figure 6. Molecular structure of Niacinamide (A) and its functional group molecules, acetamide (B), pyridine (C), and benzamide (D).

Table 9. Results of rebinding studies with compounds with different NAM functional groups

Compound	Imprinting Factor[3]	Percent Bound on MIP[4]
Pyridine[1]	2.09 ± 0.17 (8)	4.70 ± 0.39[a]
Benzamide[2]	1.92 ± 0.41 (21)	5.21 ± 1.12[a]
Acetamide[2]	1.25 ± 0.076 (6)	38.74 ± 2.34[b]
Niacinamide	2.25 ± 0.51 (23)	20.39 ± 4.65[c]

[1] Analyzed with UV Spectroscopy

[2] Analyzed with HPLC

[3] Mean of 3 replicates ± std dev (CV)

[4] Mean of 3 replicates ± std dev

There was no significant difference in the imprint factor between the pyridine, benzamide, acetamide and NAM ($p<0.0921$). There was a significant difference in percent bound in MIP between acetamide and all other molecules, as well as NAM and all other molecules. There was no significant difference between pyridine and benzamide for percent bound. According to the UV analysis, pyridine rebinding shows an imprint factor of 2.09 ± 0.17 (8.3% CV), summarized in Table 9. This suggests that the pyridine group may play an important role in rebinding of NAM to the MIP. Rebinding studies with benzamide and acetamide were analyzed using HPLC. Benzamide rebinding studies showed an imprint factor of 1.92 ± 0.41 (21.3% CV), as summarized in Table 9. As there is an imprinting effect with both benzamide and pyridine, the notion that the aromatic ring structure plays an important role in the selectivity of the rebinding is supported. However, when comparing percent bound to the MIP, benzamide (5.21 ± 1.12) may bind more strongly with the NAM imprinted polymer than pyridine

(4.70 ± 0.39) does, supporting the idea that the bulk of the structure of the NAM molecule may be necessary to have a higher percentage bound, while the pyridine ring may be responsible, at least in part, for the selectivity of the binding. This is inconclusive, though, as more replicates should be conducted in order to obtain smaller standard deviations to make the differences more significant. This is, however, further supported in literature, as it was shown that the binding capacity of pyridine and benzamide were larger on the NAM MIP than the NIP, suggesting that both the heterocyclic nitrogen and the amide group play a role in the strong recognition characteristics of the template to the functional monomer in the MIP (Fu and others 2001).

Mookda and others (2008) conducted selectivity studies using structurally related compounds to NAM, such as benzamide, pyridine, benzylamine, and acetophenone (see Figure 7). They suggested that both the pyridyl nitrogen and the amide group presence in the NAM structure play a synergistic effect in the binding specificity to the MIP, though the effect may be additive. This is because in both MIP 4 and 9 (see Table 2), pyridine (with a pyridyl nitrogen) and benzylamine (with an amine group, but no pyridyl nitrogen) showed some positive binding, while acetophenone, a structurally similar compound to NAM but with no nitrogen groups, showed negligible binding. Benzamide (also with an amide group, a carbonyl group, but no pyridyl nitrogen) showed negative binding to both polymers, which indicates that it may have self-aggregated (Mookda and others 2008).

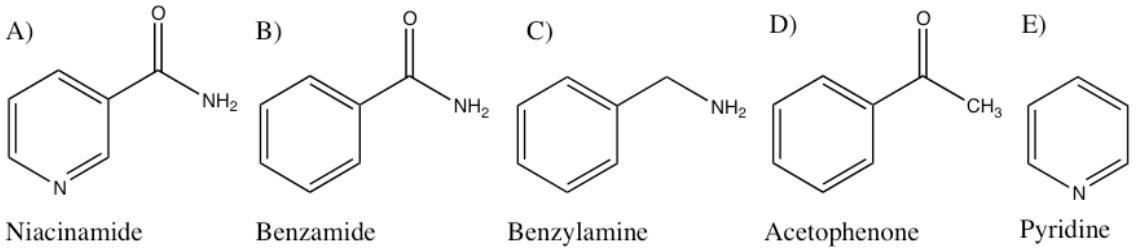

Figure 7. NAM and structurally related compounds used in Mookda and others' (2008) study: Niacinamide (A), Benzamide (B), Benzylamine (C), Acetophenone (D), Pyridine (E).

In the rebinding studies Mookda and others (2008) conducted in acetonitrile, negative values of % bound were observed in many cases. Rebinding studies were conducted by mixing a known amount of analyte with a known quantity of MIP/NIP. The absorbance of the initial amount was measured. The mixture of polymer and analyte was centrifuged and the supernatant absorbance was measured. The % bound was calculated as: [(initial absorbance – final absorbance)/initial absorbance]*100. Negative values can occur when the final absorbance is higher than the initial. It was suggested that this may be due to self-aggregation of the compound, causing an increase in the absorbance after being introduced to the polymer (Mookda and others 2008). Negative values also occurred with my benzamide and acetamide rebinding studies when measured by a UV spectrophotometer (results not included). For this reason, benzamide and acetamide were measured by HPLC, and positive values were obtained.

Li and others (2005) determined that NAM has a higher affinity than nicotinic acid with the NAM MIP. The reason for this may be due to the amide group in the NAM being able to easily form a hydrogen bond with the functional monomer compared to the acid group in the nicotinic acid. They also found that nicotinic acid binds more non-selectively with the NIP than NAM does, which leads to a lower imprint factor. This

may be due to the imprinted cavity in the MIP that has a stronger affinity for NAM because of its amide group, resulting in more NAM binding to MIP than NIP. Meanwhile, nicotinic acid will bind similarly to both the MIP and NIP in a non-selective manner (Li and others 2005). One limitation to this study is that they only studied one NAM analogue, nicotinic acid. It would be interesting to determine a competition effect with isonicotinamide, as it was previously found that the NAM MIP has a strong affinity for this molecularly similar compound.

5.6. FTIR Studies of MIPs and NIPs

FTIR spectra were taken for all polymers created to determine chemical structure characteristics. Spectra were obtained using polymers with the template removed, polymers with NAM bound, and for the monomers of EGDMA, MAA, and NAM. All FTIR polymer profiles were similar, regardless if it was an MIP with NAM as a template, or NIP. There were no significant shifts in any peaks between the MIP and NIP (see Figure 8). Therefore, the basic polymeric structure made with MAA and EGDMA, regardless of imprint, is highly likely to be similar. It also indicates reproducibility.

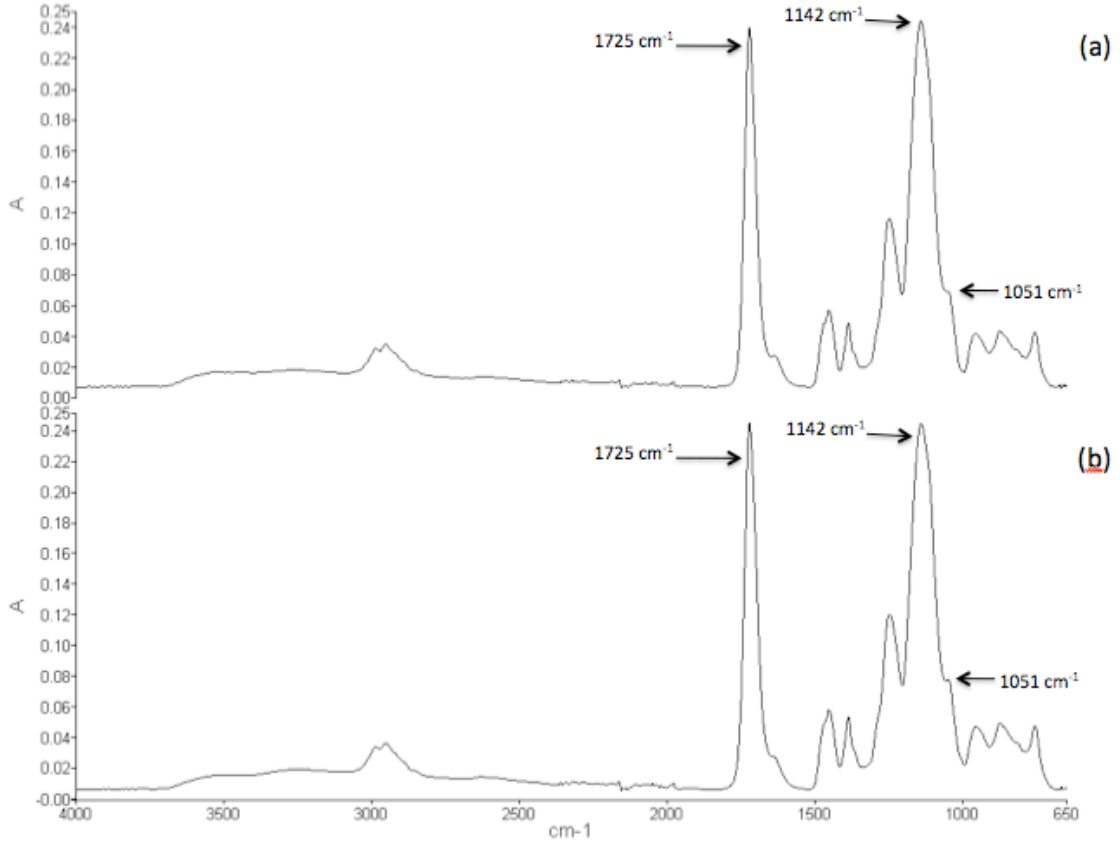

Figure 8. Comparison of FTIR Spectra of NAM MIP with NAM template removed (a) and NIP (b)

Results verified those found previously (Del Sole and others 2010), where, according to Del Sole ant others (2010), there is a peak at 1725 cm^{-1}, indicating a shift of the C=O stretching band from 1694 cm^{-1} to 1725 cm^{-1}, as well as a disappearance of a peak at 1633 cm^{-1} that indicates the deconjugation of the C=C stretch in the MAA molecule, showing that it is polymerized (Del Sole and others 2010). However, according to another source, a peak at 1725 cm^{-1} represents the C=O from the acrylate group in EGDMA (Tarducci and others 2002).

Del Sole and others (2010) failed to recognize the contribution of the spectra from EGDMA (Del Sole and others 2010). For example, the reason for the C=O shift may be partially attributed to the C=O group in EGDMA. Additionally, as shown in Figure 9, the similar peak in EGDMA is closer to the 1725 cm^{-1} peak in the MIP than it the similar peak in MAA (1717 cm^{-1} vs. 1689 cm^{-1}, respectively). Because EGDMA is in a larger proportion to MAA, its contribution to the polymer spectra should not be disregarded. It is highly likely that the wavenumber shift to 1725 cm^{-1} is due to a chemical interaction between the MAA and EGDMA, (Stuart 2004), which was not previously explained by Del Sole and others (2010).

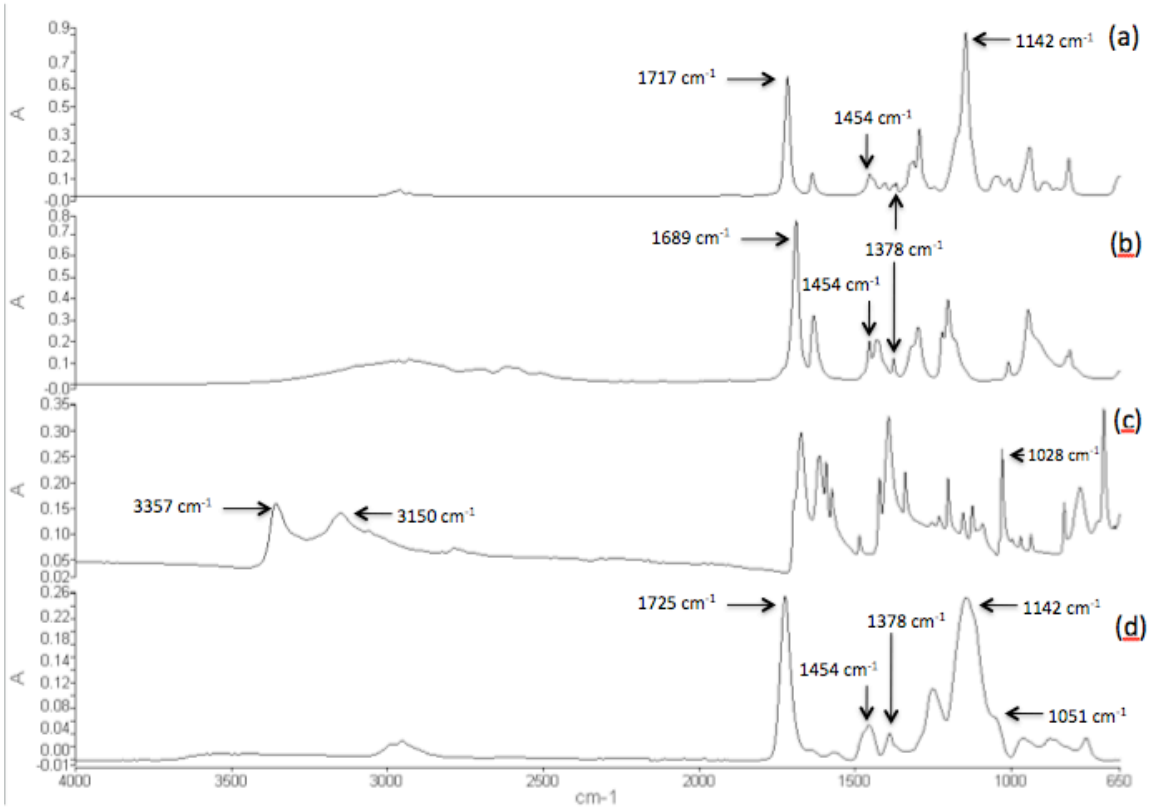

Figure 9. FTIR spectra comparison of EGDMA (a), MAA (b), NAM (c), and NAM MIP (d).

As Figure 9 illustrates, there is a peak at 1378 cm^{-1} and 1454 cm^{-1}, which both correspond to peaks that can be found on both, EGDMA and MAA FTIR spectra (Figure 9(a) and 7(b)). These peaks may represent a C—H bending in the methyl group. The peak at 1378 cm^{-1} is most probably symmetric bending and the peak at 1454 cm^{-1} is most probably antisymmetric bending (Tarducci and others 2002). As shown in Figure 10(a) and (b), both EGDMA and MAA chemical structures have a methyl group. The peaks appear to be a result of the MAA and EGDMA co-polymerization as the peak at 1378 cm^{-1} is more prominent in MAA and the peak at 1454 cm^{-1} is more defined in EGDMA. On the other hand, the 1454 cm^{-1} peak may be attributed to a CH_2 bend in the EGDMA as that typically absorbs around 1465 cm^{-1} (Glagovich 2012). In general,

wavenumber shifts and band broadening are considered indicative of chemical interactions within a blend (Stuart 2004).

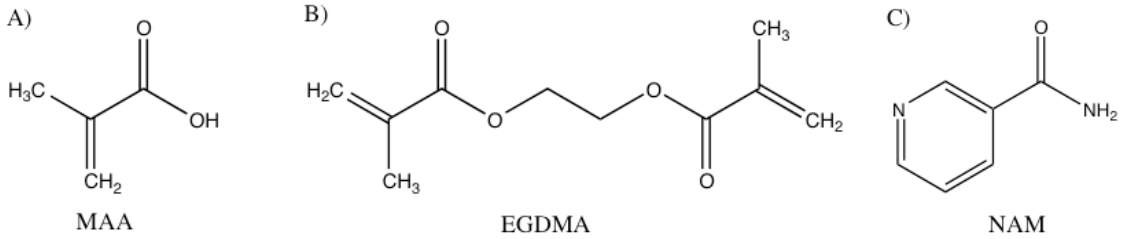

Figure 10. Chemical structure of MAA (A), EGDMA (B), and NAM (C).

Another two notable peaks illustrated in Figure 9(c) are those at 3357 cm^{-1} and 3150 cm^{-1}. These peaks represent asymmetric and symmetric stretching of the NH_2 group in NAM, respectively (Bayari and others 2003). Hypothetically, it could be possible to quantify NAM bound to the MIP using this signal (Stuart 2004). However, more research needs to be conducted to determine the feasibility of this method of quantification for NAM.

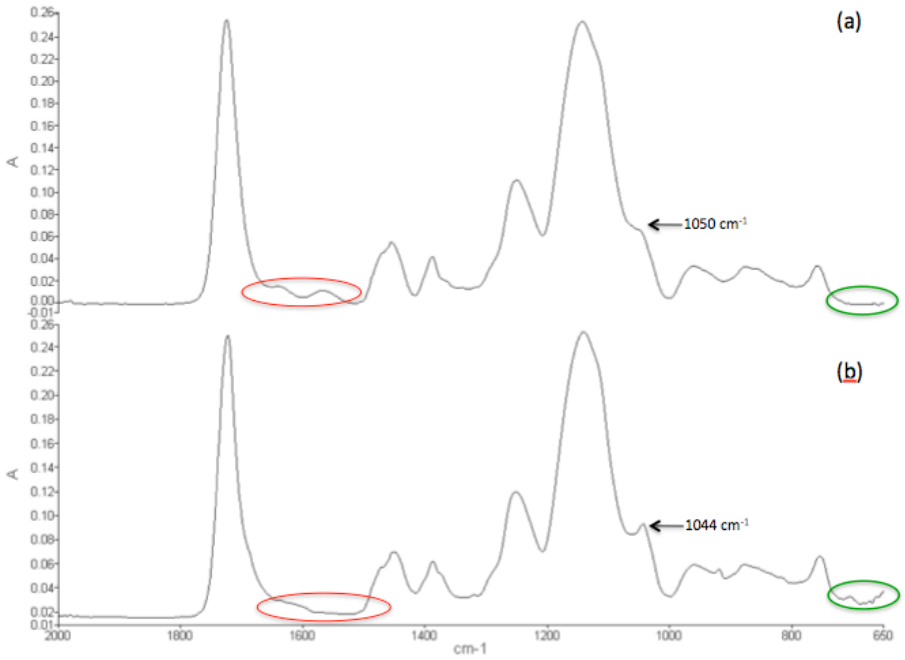

Figure 11. Comparison of 1:4 MAA:EGDMA MIP with no free NAM (a) and NAM in excess to the amount bound (b).

Another possibility for quantification of NAM using FTIR and the MIP lies with the region at 1044 cm^{-1}. A shoulder noted in the spectra of the MIP with no free NAM (Figure 11a) at 1050 cm^{-1} was shifted to a distinct peak at 1044 cm^{-1} when NAM was bound (Figure 11b). It is also known that at 1028 cm^{-1}, a peak is characteristic of stretching of pyridine in NAM (Bayari and others 2003), as shown in Figure 9(c). Therefore, it may be that the peak at 1044 cm^{-1} is representative of NAM, shifted due to vibrational changes from interactions with the polymer.

Other notable areas of the spectra in Figure 9 are the regions between 1700 cm^{-1} and 1500 cm^{-1}, as well as the between 700 cm^{-1} and 650 cm^{-1}. In the former, the spectra with the free NAM (Figure 11(b)) has no significant peaks while the spectra with no free NAM has peaks. ^{1}H-NMR studies conducted with the monomers showed that the interactions between NAM and MAA were not ionic in nature (Del Sole and others

2009). Therefore, the hydrogen bonding interactions may play a role in suppressing the peaks in the 1700 cm^{-1} to 1500 cm^{-1} region. Meanwhile, in the latter region (700 cm^{-1} to 650 cm^{-1}) there are small peaks, which may be indicative of free NAM. It has been found that activity in the 700 to 640 cm^{-1} region is indicative of outer and inner plane ring deformation, respectively, of the pyridyl structure otherwise known as ring puckering (Bayari and others 2003). It is important to note that NAM may have to bind in a higher quantity to be quantified by FTIR analysis.

The polymers of different ratios of MAA:EGDMA were analyzed with FTIR to determine any structural differences and are illustrated in Figure 12. The spectra were all fairly similar except for two significant differences. The first that was noted was that once the ratio is less than 1:3 MAA:EGDMA, the peak at 1724 cm^{-1} is less broad and more defined as seen in Figures 12 (d-g). The base of the peak starts at around 1860 cm^{-1} and ends at around 1690 cm^{-1}. It has been found that bands within this region for polymers with similar chemical composition correspond to vibrations of free and bonded ester groups in both ordered and disordered forms (Bozena 1998). Therefore, the larger peak may be a composition of these vibrations. The region around 1698 cm^{-1} corresponds to the bonded ester groups, which indicates why there is a broader plateau or shoulder on the peak in Figures 12 (a-c), because there is less EGDMA available and most of it, if not all, is bonded with the MAA. On the other hand, in the other spectra, there is more EGDMA and therefore, more free ester groups leading to a clearer peak.

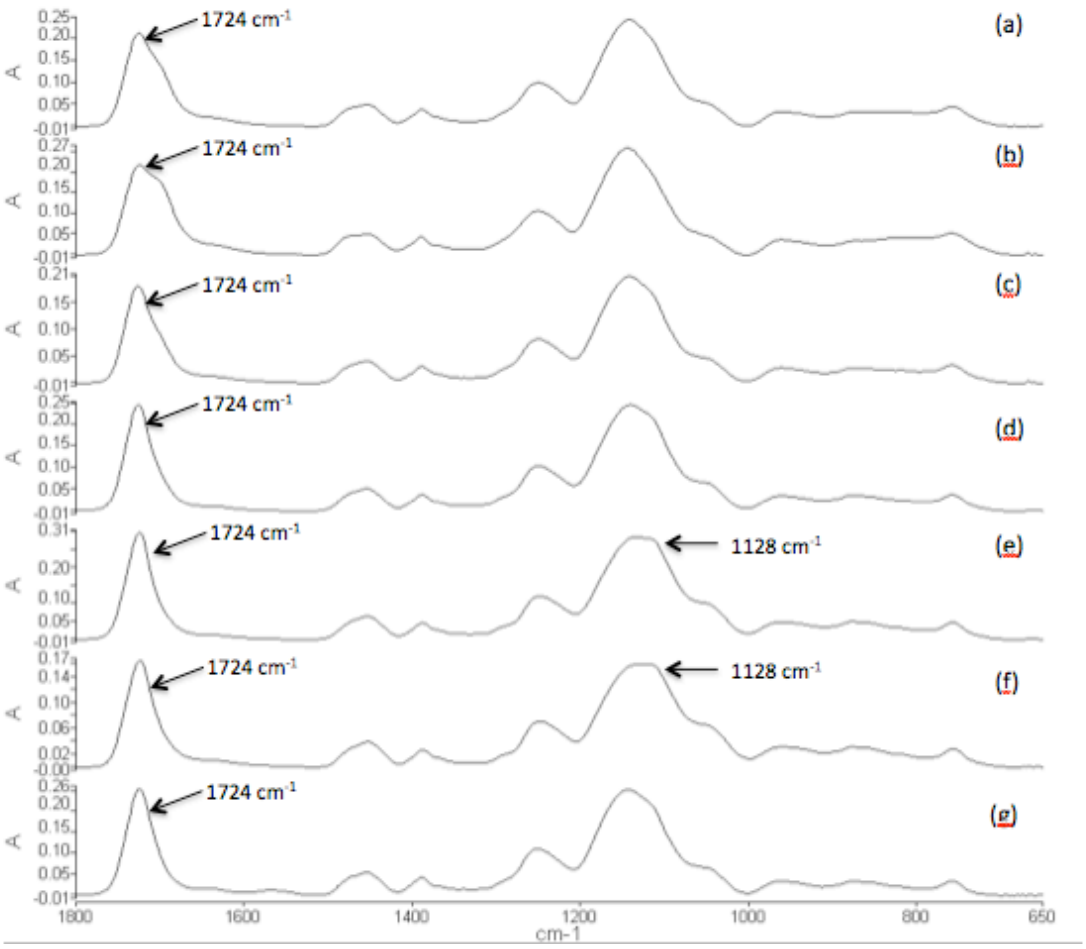

Figure 12. Comparison of FTIR spectra between 1:0.75 MAA:EGDMA MIP (a), 1:1.25 MIP (b), 1:2 MIP (c), 1:3 MIP (d), 1:5 MIP (e), 1:6 MIP (f), 1:4 MIP (g).

The second difference noticed in the spectra in Figures 12 (a-g) was the peak at 1142 cm^{-1}. As the ratio of MAA:EGDMA gets smaller, indicating higher proportion of EGDMA, the peak broadens and is indicated at 1128 cm^{-1}. This further supports that the peak at 1142 cm^{-1} can be ascribed to chemical interactions between MAA and EGDMA as suggested by previous work. It was also previously suggested that the peak at 1142 cm^{-1} is due to the C—O stretching of a carboxylic acid (Del Sole and others 2010). However, as Figure 9 and Figure 12 support, this peak is characteristic of EGDMA and may in fact be due to the C—O stretching in the ester linkage of the molecule (Tarducci and others 2002).

One of the goals of this study was to be able to determine a chemical structure for the MIP obtained. In a previous paper, the binding possibilities and binding energies of MAA to NAM were determined computationally (Wu and others 2003). Four different binding formations were suggested for NAM and MAA are in a 1:1 ratio. In the 1:1 complexes, it was found that there is a strong difference in strength of the hydrogen bonds between the two molecules at the four different binding sites. The double hydrogen bond between carboxyl group of MAA and the amide group of NAM was the most stable. Conversely, the hydrogen bond between the carbonyl oxygen in MAA and the amidic proton in NAM had the weakest stabilization energy (Del Sole and others 2009).

As the ratio between NAM:MAA is not 1:1 during polymerization, the research group also developed schematics of pre-polymerization complexes for a 1:2, 1:3, and 1:4 ratio. Having excess MAA may provide more stability for the NAM-MAA interaction. MAA also has hydrogen bonds with other MAA molecules, which makes the complex more stable (Del Sole and others 2009). However, when comparing the literature results to the obtained experimental FTIR spectra for the different MAA:EGDMA ratio polymers, particularly between the 1:2, 1:3, and 1:4 MAA:EGDMA spectra, it was noticed that the peak at 1724 cm^{-1} was broader in the 1:2 ratio, but narrower for all other ratios where EGDMA is higher. This shows that a sharper peak in this region may be related to a more stable pre-polymerization complex.

5.7. Scanning Electron Microscopy Imaging

Scanning electron microscopy was used to characterize the morphology of the MIPs and potentially obtain information about the physical structure of the polymer.

Unfortunately, it was difficult to gather conclusive information about the polymer pore size distribution without another analysis, such as with a porosimeter. Images were obtained for 1:4 MAA:EGDMA MIP (Figure 13) and NIP (Figure 14), as well as the 1:0.75 MAA:EGDMA MIP (Figure 15). No conclusive differences could be stated between the 1:4 MAA:EGDMA MIP (Figure 13) and NIP (Figure 14) based on the SEM images. However, both do appear to have an amorphous surface with possible cavities for NAM to bind to. There is an obvious difference in surface appearance between the 1:4 MAA:EGDMA MIP/NIP and the 1:0.75 MAA:EGDMA MIP (Figure 15). In Figure 15, it appears that the polymer has less pores or cavities. However, as seen before in Table 9, the percent bound of the 1:0.75 MAA:EGDMA polymers were much higher than the 1:4 MAA:EGDMA polymer.

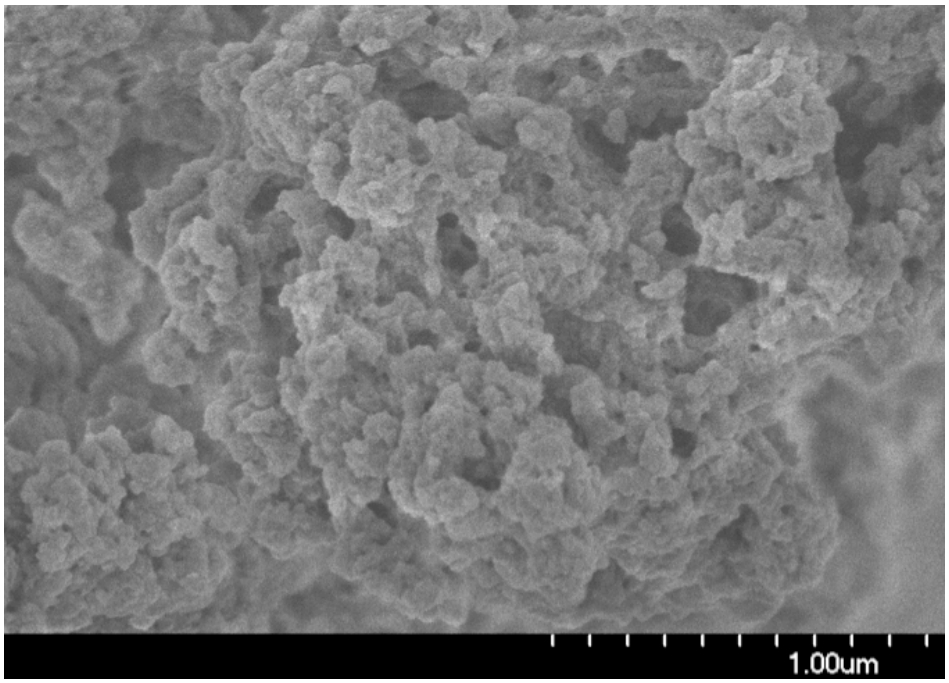

Figure 13. SEM image of a 1:4 MAA:EGDMA MIP, at 50000x magnification.

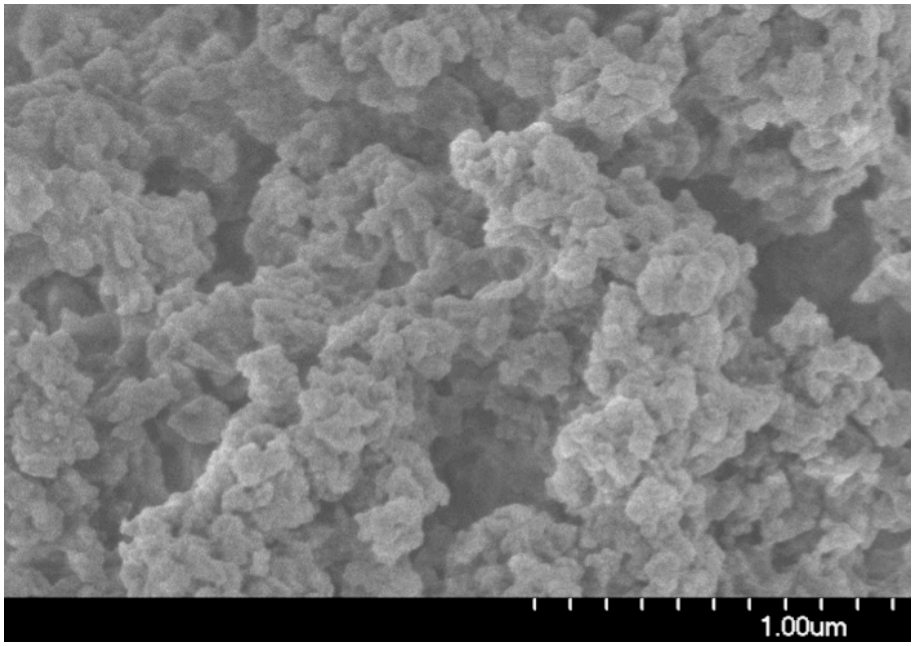

Figure 14. SEM image of a 1:4 MAA:EGDMA NIP, at 50000x magnification.

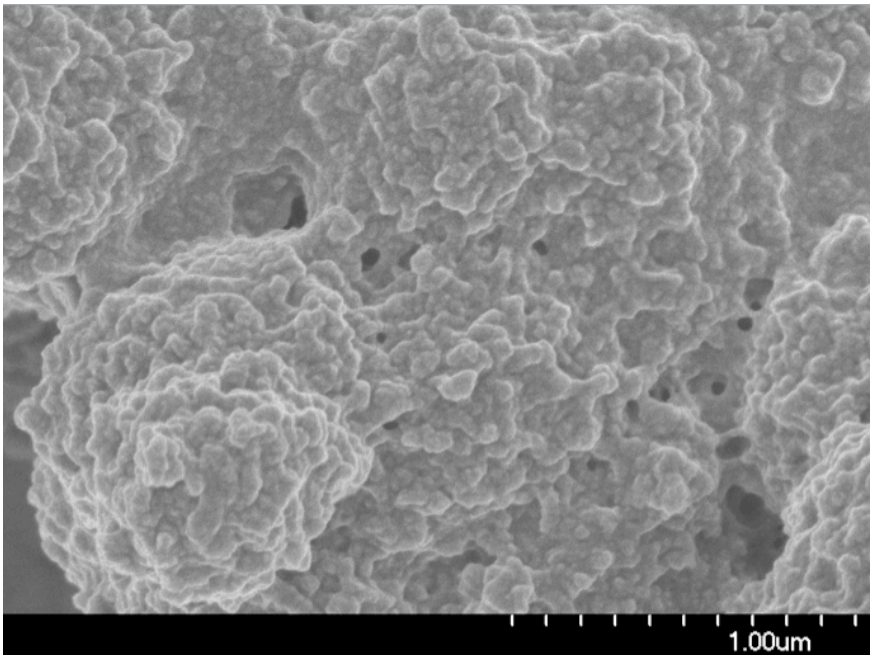

Figure 15. SEM image of a 1:0.75 MAA:EGDMA MIP, at 50000x magnification.

Therefore, the porosity may not affect percent of NAM bound, but rather the amount of surface area with functional groups affects it.

Mookda and others (2008) also obtained SEM images for their optimal MIP, which was the 1:1 MAA:TRIM polymer. It was found that the crushed polymers had an irregular shape containing a rough surface, possibly similar to that in Figure 13 and 14. However, the SEM images from that research were not with a high enough magnification to gather surface characteristics information. They were able to determine that their size range of polymer particles was between 5-15 μm. Further morphology was not conducted on the polymer (Mookda and others 2008). Another limitation of this obtained size range was that the polymers were not put through a sieve to gain particle size uniformity. Nor was it described how the polymer was crushed. Therefore, it is likely that the size measured is highly subjective to the limits of the SEM. On the other hand, Del Sole and others (2007) obtained SEM images for their MIP microspheres, imprinted with 1,8-diazabicyclo[5.4.0]undec-7-ene (DBU). Although the magnification strength was not indicated in the article, they were able to identify spherical MIP microparticles to be (10 ± 43) μm, while the NIP microspheres were (18 ± 3) μm showing a much narrower particle size distribution. The MIP microspheres had a wider size distribution than the NIP (Del Sole and others 2007), which is potentially indicative of the DBU template creating pores or cavities making the microspheres more voluminous. It would be beneficial to generate and characterize uniform particles as opposed to crushed polymer agglomerate to gain a better idea of pore sizes. This would also be ideal for understanding particle size for column packing if the MIP were to be used as a solid phase extraction matrix.

Chapter 6. Conclusions and Future Work

6.1. Study Findings

This study has shown that a MIP can be successfully synthesized to selectively bind NAM using a 1:4 ratio of MAA:EGDMA with chloroform as the porogen and AIBN as the free radical initiator with an imprint factor of 2.37 ± 0.10. It was shown that the amount of AIBN used had no significant effect on the polymer selectivity and amount of analyte rebinding within 0.1 g to 0.3 g AIBN range. This study further supported that the structure of the entire NAM molecule including the amide group and the pyridyl nitrogen were critical in binding and selectivity of the polymer via hydrogen binding. Characteristic peaks were determined in FTIR spectra for the structure of the MIP and NIP. Results supported much of that found in FTIR analysis by Del Sole and others (2010), except that the peak at 1725 cm^{-1} is more likely due to EGDMA from ordered and disordered bonded ester groups, rather than MAA. The peak at 1378 cm^{-1} is correlated with symmetric bending and the peak at 1453 cm^{-1} is due to antisymmetric bending of the CH_3 group in the polymer. Certain peaks were attributed to residual NAM in the MIP, leading to the possibility of quantifying NAM via FTIR analysis, such as the shoulder at 1044 cm^{-1}, as well as the regions between 1500 – 1700 cm^{-1} and 650 – 700 cm^{-1}. It was also determined that the peak at 1142 cm^{-1} was due to C—O stretching in the ester group of EGDMA rather than the carboxylic acid in MAA as stated previously by Del Sole and others (2010). SEM images of 1:4 MAA:EGDMA MIP and NIP, and 1:0.75 MAA:EGDMA MIP showed that the polymers have a rough, amorphous surface.

However, the 1:0.75 MAA:EGDMA polymer appeared to be less porous and more dense than the 1:4 MAA:EGDMA polymers.

6.2. Future Studies

Due to time constraints, it was difficult to conduct more rebinding studies with more molecularly similar compounds to NAM to gather more information about MIP selectivity and rebinding mechanisms. It would be beneficial to conduct rebinding studies with compounds such as benzene, pyrazinamide, thionicotinamide, and nicotine, as well as other compounds previously investigated by other researchers for verification. This would help gather more conclusive data about rebinding mechanisms and selectivity.

Another area to be investigated could be the potential of NAM quantification in the MIP using FTIR analysis. It was determined that the peaks at 3357 and 3150 cm^{-1} most likely correspond to NAM bound in the polymer, as well as a shoulder at 1044 cm^{-1} and the region between 650 – 700 cm^{-1}. Theoretically, if the spectra of the polymer with NAM rebound to it were subtracted by the spectra of the polymer with NAM removed completely from it, NAM could be quantified via a standard curve. However, it may be beneficial to create a polymer with a higher percentage of binding so that it can be detected more strongly in the FTIR spectra.

Using the SEM images, it was difficult to characterize the porosity of the polymer without the supplementation of other analyses for pore sizes such as using a porosimeter. The use of the porosimeter was scheduled for this study. However, due to technical difficulties and time constraints, this analysis was not feasible. Therefore, it is

recommended for continuity of this study that pore sizes of the polymer be investigated and quantified as a supplement to SEM images.

One of the original objectives of this study was to determine the feasibility of using an MIP in a microfluidic chip. Therefore, as a part of the continuity of this study, this aspect will be further investigated. It will need to be determined whether the MIP within the microfluidic channel would be best suited as packing material or ligated onto the surface of the channel using a surface modification technique.

Bibliography

Association of Official Analytical Chemists International. 1998a. AOAC Official Method 961.14, Niacin and Niacinamide in Drugs, Foods, and Feeds, Colorimetric Method. In: Official Methods of Analysis of AOAC International. 16th ed. AOAC International. p 45.1.10.

Association of Official Analytical Chemists International. 1998b. AOAC Official Method 975.41, Niacin and Niacinamide in Cereal Products, Automated Method. In: Official Methods of Analysis of AOAC International. 16th ed. AOAC International. p 45.1.11.

Association of Official Analytical Chemists International. 1998c. AOAC Official Method, 981.16, Niacin and Niacinamide in Foods, Drugs, and Feeds, Automated Method. In: Official Methods of Analysis of AOAC International. 16th ed. AOAC International. p 45.1.12.

Association of Official Analytical Chemists International. 1998d. AOAC Official Method 968.32, Niacinamide in Multivitamin Preparations, Spectrophotometric Method. In: Official Methods of Analysis of AOAC International. 16th ed. AOAC International. p 45.1.13.

Association of Official Analytical Chemists International. 1998e. AOAC Official Method 944.13, Niacin and Niacinamide (Nicotinic Acid and Nicotinamide) in Vitamin Preparations, Microbiological Method. In: Official Methods of Analysis of AOAC International. 16th ed. AOAC International. p 45.2.04.

Association of Official Analytical Chemists International. 1998f. AOAC Official Method 960.46 Vitamin Assays, Microbiological Methods. In: Official Methods of Analysis of AOAC International. 16th ed. AOAC International. p 45.2.01.

Atalay YT, Vermeir S, Witters D, Vergauwe N, Verbruggen B, Verboven P, Nicolaï BM, Lammertyn J. 2011. Microfluidic analytical systems for food analysis. Trends Food Sci.Technol. 22(7):386-404.

Aurora Prado MS, Steppe M, Tavares MFM, Kedor-Hackmann ERM, Santoro MIRM. 2005. Comparison of capillary electrophoresis and reversed-phase liquid chromatography methodologies for determination of diazepam in pharmaceutical tablets. J. Pharm. Biomed. Anal. 37(2):273-9.

Bayari S, Atac A, Yurdakul S. 2003. Coordination behaviour of nicotinamide: an infrared spectroscopic study. J. Mol. Struct. 655(1):163-70.

Beltran A, Borrull F, Cormick PAG, Marce RM. 2010. Molecularly-imprinted polymers: useful sorbents for selective extractions. Trends. Anal. Chem. 29(11):1363-75.

Blasco AJ, Barrigas I, González MC, Escarpa A. 2005. Fast and simultaneous detection of prominent natural antioxidants using analytical microsystems for capillary electrophoresis with a glassy carbon electrode: A new gateway to food environments. Electrophoresis 26(24):4664-73.

Bozena K. 1998. FTIR study of hydrogen bonds in aliphatic polyesteramides. Polymer 39(23):5853-60.

Brazier JJ, Yan M. 2005. Micromonoliths and Microfabricated Molecularly Imprinted Polymers. In: Mingdi Yan, Olof Ramstrom, editors. Molecularly Imprinted Materials: Science and Technology. 1st ed. New York, NY: Marcel Dekker. p 491-516.

Capella-Peiró M, Carda-Broch S, Monferrer-Pons L, Esteve-Romero J. 2004. Micellar liquid chromatographic determination of nicotinic acid and nicotinamide after precolumn König reaction derivatization. Anal. Chim. Acta 517(1-2):81-7.

Chemical Compatibility Database [Internet]. Montreal, Canada: Cole Parmer, Inc.; 2011 [Accessed 2011 December 14]. Available from: http://www.coleparmer.com/Chemical-Resistance

Cormack PAG, Elorza AZ. 2004. Molecularly imprinted polymers: synthesis and characterisation. J. Chromatogr. B 804(1):173-82.

Crevillén AG, Blasco AJ, González MC, Escarpa A. 2006. A fast and reliable route integrating calibration and analysis protocols for water-soluble vitamin determination on microchip-electrochemistry platforms. Electrophoresis 27(24):5110-8.

Del Sole R, Lazzoi MR, Vasapollo G. 2010. Synthesis of nicotinamide-based molecularly imprinted microspheres and in vitro controlled release studies. Drug Delivery 17(3):130-7.

Del Sole R, Scardino A, Lazzoi MR, Vasapollo G. 2011. Molecularly imprinted polymer for solid phase extraction of nicotinamide in pork liver samples. J. of Appl. Polym. Sci. 120(3):1634-41.

Del Sole R, De Luca A, Catalano M, Mele G, Vasapollo G. 2007. Noncovalent imprinted microspheres: Preparation, evaluation, and selectivity of DBU template. J. Appl. Polym. Sci. 105(4):2190-7.

Del Sole R, Lazzoi MR, Arnone M, Sala FD, Cannoletta D, Vasapollo G. 2009. Experimental and Computational Studies on Non-Covalent Imprinted Microspheres as Recognition System for Nicotinamide Molecules. Molecules 14(7):2632-49.

Eitenmiller RR, Landen Jr. WO. 1999. Chapter 9: Niacin. In: Anonymous Vitamin Analysis for the Health and Food Sciences. Boca Raton, FL: CRC Press. p 339-67.

Escarpa A, González MC, Crevillén AG, Blasco AJ. 2007. CE microchips: An opened gate to food analysis. Electrophoresis 28(6):1002-11.

Fu Q, Zheng N, Li YZ, Chang WB, Wang ZM. 2001. Molecularly imprinted polymers from nicotinamide and its positional isomers. J. Mol. Recognit. 14(3):151-6.

Fuentes HV. 2007. Microchip Liquid Chromatography and Capillary Electrophoresis Separations in Multilayer Microdevices. [dissertation]. Provo, UT, USA: Brigham Young University.

Glagovich [internet]. New Britain, CT: Central Connecticut State University; 2012. [Accessed 2012 Aug 29]. Available from http://www.chemistry.ccsu.edu/glagovich/teaching/316/ir/table.html.

Goodwin JW, Harbron RS, Reynolds PA. 1990. Functionalization of colloidal silica and silica surfaces via silylation reactions. Colloid. Polym. Sci. 268(8):766-77.

Grover WH, Skelley AM, Liu CN, Lagally ET, Mathies RA. 2003. Monolithic membrane valves and diaphragm pumps for practical large-scale integration into glass microfluidic devices. Sens. Actuators, B. 89(3):315-23.

Harris CM. 2003. Shrinking the LC landscape. Anal. Chem. 75(3):64A-69.
He B, Tait N, Regnier F. 1998. Fabrication of nanocolumns for liquid chromatography. Anal. Chem. 70(18):3790-7.

Holland N. 2008. An Investigation into the Role of Morphology on the Performance of Molecularly Imprinted Polymers. [dissertation]. Waterford, Ireland: Waterford Institute of Technology. 5 p.

Hong C, Chang P, Lin C, Hong C. 2010. A disposable microfluidic biochip with on-chip molecularly imprinted biosensors for optical detection of anesthetic propofol. Biosens. Bioelectron. 25(9):2058-64.

Huang SC, Lee GB, Chien FC, Chen SJ, Chen WJ, Yang MC. 2006. A microfludic system with integrated molecular imprinting polymer films for surface plasmon resonance detection. J. Micromech. Microeng. 16(7):1251-7.

Jaggi N, Vij DR. 2006. Fourier Transform Infrared Spectroscopy. In: Anonymous Handbook of Applied Solid State Spectroscopy. New York, NY: Springer US. p 411-50.

Jemere AB, Oleschuk RD, Harrison DJ. 2003. Microchip-based capillary electrochromatography using packed beds. Electrophoresis. 24(17):3018-25.

Kirsch N, Whitcombe MJ. 2005. The Semi-Covalent Approach. In: Mingdi Yan, Olof Ramstrom, editors. Molecularly Imprinted Materials: Science and Technology. New York, NY: Marcel Dekker. p 93-122.

Li Z, Yang G, Liu S, Chen Y. 2005. Adsorption isotherms on nicotinamide-imprinted polymer stationary phase. J. Chromatogr. Sci. 43(7):362-6.

Lutz BR, Chen J, Schwartz DT. 2003. Microfluidic without Microfabrication. Proc. Natl Acad. Sci. 100(8):4395-8.

Mayes Research Group [internet]. Norfolk, UK: University of East Anglia; n.d. [Accessed 2012 Aug 14]. Available from http://www.uea.ac.uk/~c016/research.htm.

Mookda P, Singha K, Weeranuch K, Chatchai T. 2008. Synthesis of nicotinamide-imprinted polymers and their binding performances in organic and aqueous media. e-Polymers 91:1-9.

Oleschuk RD, Shultz-Lockyear LL, Ning Y, Harrison DJ. 2000. Trapping of bead-based reagents within microfluidic systems: On-chip solid-phase extraction and electrochromatography. Anal. Chem. 73(3):585-90.

Prasad BB, Tiwari K, Singh M, Sharma PS, Patel AK, Srivastava S. 2008. Molecularly imprinted polymer-based solid-phase microextraction fiber coupled with molecularly imprinted polymer-based sensor for ultratrace analysis of ascorbic acid. J. Chromatogr. A. 1198-1199:59-66.

Ramstrom O. 2005a. Molecular Imprinting--An Introduction. In: Mingdi Yan, Olof Ramstrom, editors. Molecularly Imprinted Materials: Science and Technology. New York, NY: p 1-12.

Ramstrom O. 2005b. Synthesis and Selection of Functional Monomers. In: Mingdi Yan, Olof Ramstrom, editors. Molecularly Imprinted Materials: Science and Technology. 1st ed. New York, NY: Marcel Dekker. p 181-224.

Reuhs BL, Rounds MA. 2010. High-Performance Liquid Chromatography. In: S. Suzanne Nielsen, editor. Food Analysis. 4th ed. ed. New York, NY: Springer Science + Business Media, LLC. p 499-512.

Sato K, Hibara A, Tokeshi M, Hisamoto H, Kitamori T. 2003. Microchip-based chemical and biochemical analysis systems. Adv. Drug Delivery Rev. 55(3):379-91.

Scampicchio M, Wang J, Mannino S, Chatrathi MP. 2004. Microchip capillary electrophoresis with amperometric detection for rapid separation and detection of phenolic acids. J. Chromatogr. A. 1049(1-2):189-94.

Schmitt-Kopplin P, Fekete A. 2007. The CE Way of Thinking. In: Philippe Schmitt-Koplen, editor. Capillary Electrophoresis: Methods and Protocols. Totowa, NJ, USA: Humana Press. p 611-29.

Serwe M. 2000. A comparison of CE-MS and LC-MS for peptide samples. LC-GC 18(1):46-51.

Slentz BE, Penner NA, Lugowska E, Regnier F. 2001. Nanoliter capillary electrochromatography columns based on collocated monolithic support structures molded in poly(dimethyl siloxane). Electrophoresis 22(17):3736-43.

Stachowiak TB, Rohr T, Hilder EF, Peterson DS, Yi M, Svec F, Frechet JMJ. 2003. Fabrication of porous polymer monoliths covalently attached to the walls of channels in plastic microdevice. Electrophoresis. 24(21):3689-93.

Stein J, Hahn A, Rehner G. 1995. High-performance liquid chromatographic determination of nicotinic acid and nicotinamide in biological samples applying post-column derivatization resulting in bathmochrome absorption shifts. J. Chromatogr. B: Biomedical Sciences and Applications 665(1):71-8.

Stratigos JD, Katsambas A. 2006. Pellagra: a still existing disease. Brit. J. Dermatol. 96(1):99-106.

Stuart B. 2004. Infrared Spectroscopy: Fundamentals and Applications. Hoboken, NJ, USA: Wiley. 244 p.

Tamayo FG, Turiel E, Martín-Esteban A. 2007. Molecularly imprinted polymers for solid-phase extraction and solid-phase microextraction: Recent developments and future trends. J. Chromatogr. A 1152(1-2):32-40.

Tarducci C, Schofield WCE, Badyal JPS. 2002. Synthesis of cross-linked ethylene glycol dimethacrylate and cyclic methacrylic anhydride polymer structures by pulsed plasma deposition. Macromolecules 35(23):8724-7.

Ward CM, Trenerry VC. 1997. The determination of niacin in cereals, meat and selected foods by capillary electrophoresis and high performance liquid chromatography. Food Chem. 60(4):667-74.

Wu L, Li Y. 2004. Study on the recognition of templates and their analogues on molecularly imprinted polymer using computational and conformational analysis approaches. J. Mol. Recognit. 17(6):567-74.

Wu L, Sun B, Li Y, Chang WB. 2003. Study properties of molecular imprinting polymer using a computational approach. Analyst 128:944-9.

Wu L, Zhu K, Zhao M, Li Y. 2005. Theoretical and experimental study of nicotinamide molecularly imprinted polymers with different porogens. Anal. Chim. Acta 549(1-2):39-44.

Wulff G. 2005. The Covalent and Other Stoichiometric Approaches. In: Mingdi Yan, Olof Ramstrom, editors. Molecularly Imprinted Materials: Science and Technology. New York, NY: Marcel Dekker. p 59-92.

Ye L, Mosbach K. 2001. Molecularly imprinted microspheres as antibody binding mimics. React. Funct. Polym. 48(1-3):149-157.

Yilmaz E, Schmidt RH, Mosbach K. 2005. The Noncovalent Approach. In: Mingdi Yan, Olof Ramstrom, editors. Molecularly Imprinted Materials: Science and Technology. New York, NY: Marcel Dekker. p 25-57.

Zhang Z, Li H, Liao H, Nie L, Yao S. 2005. Influence of cross-linkers' amount on the performance of piezoelectric sensor modified with molecularly imprinted polymers. Sens. Actuators, B. 105(2):176-182.

Appendix

A mel-*co*-chl Polymer with L-AA Template

The original intention for my research was to create a solid phase extraction (SPE) system in microfluidic chips for food analysis, using the principles for molecularly-imprinted polymer (MIP) demonstrated by Prasad and others (2008), and using capacitively-coupled contactless conductivity for detection.

A. Summary of original experimental design

In the first objective of the project, the aim was to bind the MIP created based on Prasad and others' (2008) work to a PMMA support. The modified protocol for the MIP synthesis, and binding MIP to PMMA is described in sequence in Figure 16. Once the protocol had been established, the next part was to optimize the binding capacity of the mel-*co*-chl polymer by assaying polymers created from various ratios of the monomers. The second objective was to determine optimal design of the microfluidic chip.

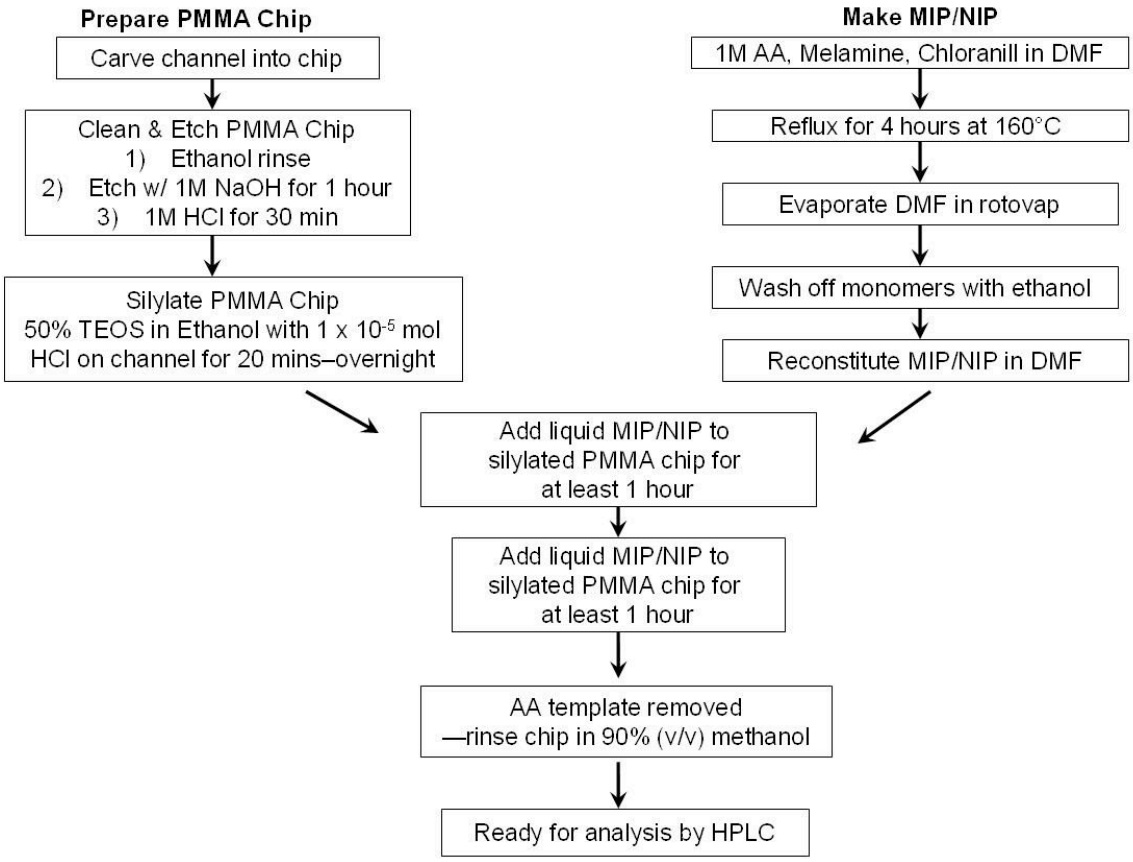

Figure 16. Summary of L-AA MIP synthesis procedure. PMMA--polymethyl methacrylate; TEOS--tetraethyl orthosilicate; DMF--dimethylformamide

B. Results Review

Two columns in two different PMMA chips were hand-carved, silylated, and bound with ascorbic acid molecularly imprinted polymer (AA-MIP). Positive results would indicate more L-AA detected by HPLC in the final 90% methanol elution than in the original rinse with H_2O after the L-AA has bound to the molecularly-imprinted polymer (MIP) from the standard. As shown in Table 10, the area under the curve, or the peak, of the RP-HPLC graph was significantly larger for both replicates in the 90%

methanol elution than the rinse with H_2O after the L-AA has bound by a factor of approximately 5 and 7 for Trial 1 and Trial 2, respectively.

Table 10. Area under RP-HPLC curve for L-AA determination in MIP and non-modified PMMA chip

Trial #	Sample	MIP-PMMA	Non-modified PMMA
Trial 1	H_2O rinse	7	0
	MeOH elution	51	11
Trial 2	H_2O rinse	448	NA
	MeOH elution	2156	NA

Though these results are not suitable for quantification, they indicate that the MIP has successfully bound to the silylated PMMA and could effectively reversibly bind L-AA after its template has been removed.

C. Issues with mel-*co*-chl polymer

1. Attachment of polymer to glass

Polymer attachment to glass lamelles was attempted by etching according to Prasad and others (2008), as well as using a stronger etching procedure involving nitric acid (Goodwin and others 1990). The MIP in dimethylformamide (DMF), the porogen, was added to silylated lamelles. Visual inspection of the chips showed some slight modification of the glass, outlining the edges of where the MIP solution was added. However, HPLC analysis of the L-AA assay on the lamelles showed no binding of L-AA,

and possibly no binding of the polymer with Prasad and others' (2008) method. With the stronger etch, it was visually evident that no polymer had bound to the glass.

2. Attachment of polymer to other PMMA sources

Polymer attachment to another source of PMMA was attempted by etching and silylating PMMA cuvettes. However, cuvettes dissolved when exposed to DMF. Another PMMA material, Plaskolite Optix, was purchased from Acrylco in New Westminster, Canada, and was created into small assay chips containing 15 wells (see Figure 17). In an assay, each well was etched and silylated using the previous procedure (Prasad and others 2008) and MIP or non-imprinted polymer (NIP, polymer without L-AA template) was added to each well and left overnight. However, assay results were inconsistent with this method. Initially, it did not appear that the polymers were coating the wells evenly as, when the black, dried unbound polymers were removed, the wells still sometimes looked as translucent white as the original chip, indicating that there was probably no polymer bound to the well.

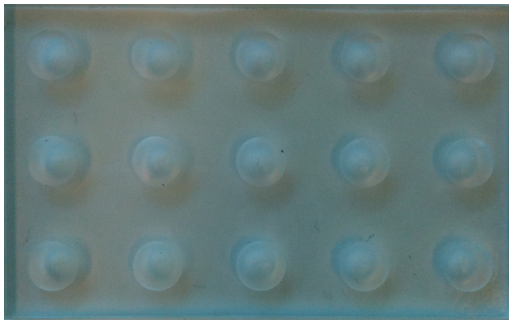

Figure 17. PMMA Assay Chips, each well with diameter of 5 mm and depth of 2.5 mm.

When the assay was conducted by heating the PMMA chip with a hotplate while adding the MIP and NIP to the wells, binding appeared to be better as shown by an even brown coating of polymer on the wells after the excess MIP and NIP was removed (see

Figure 18). However, it was evident that the MIP bound better than the NIP, as the NIP wells appeared whiter and unevenly coated than the MIP wells.

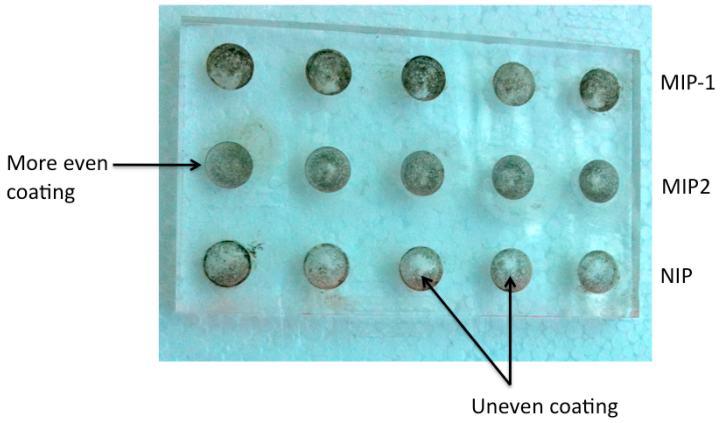

Figure 18. PMMA wells coated with L-AA mel-*co*-chl MIP and NIP.

3. Different rinsing procedures in assay

The original rinsing procedure conducted was as outlined in Prasad and others (2008). For the assay, after the loosely bound MIP had been removed, each well was rinsed well with 90% methanol in H_2O three times with a pipette to remove the L-AA template. The last rinse was collected for analysis with HPLC to indicate there was no template left on the polymer. Standard 1M L-AA solution in H_2O was added to each well for 15 minutes and was subsequently rinsed well with distilled, deionized water by soaking and agitating for 30 minutes. The last rinse was collected for analysis with HPLC to indicate that all unbound L-AA had been rinsed off. In the last step, L-AA bound to the polymer was eluted with 90% methanol in water and collected for HPLC analysis. This rinsing procedure often resulted in higher yield with the water rinse, than with the 90% methanol elution as can be seen Table 11.

Table 11. L-AA assay with mel-*co*-chl MIP using two different rinsing procedures.

	Amount of L-AA (nanogram)	
	Original Rinsing Procedure[1]	**Reverse Rinsing Procedure[2]**
L-AA Template Removal	0	0
Rinse	385 ± 28	38 ± 3
L-AA Elution	14 ± 1	4 ± 1

[1] Original rinsing procedure indicates method from Prasad and others (2008) where template and elution are conducted with 90% methanol, and rinsing of excess L-AA standard is with H_2O

[2] Reverse rinsing procedure indicates L-AA template removal and elution are conducted with H_2O and rinse of excess L-AA standard is with 90% methanol

The basis for re-binding of the template to the MIP is hydrogen bonding and ionic forces. Since water is a more polar solvent than methanol, the rinsing procedure was reversed from rinsing with water and then a 90% methanol elution to rinsing with 90% methanol and eluting with water. Additionally, the template removal step was also done with H_2O. However, as can be seen in Table 2, there is no significant difference between the two rinsing procedures in terms of improving the elution yield. Both procedures yielded a higher amount in the L-AA rinse and a lower amount of L-AA in the elution step, possibly indicating low binding or, majority of the L-AA removal during the rinsing step. It may be noted, however, that the original rinsing procedure yielded higher quantities of L-AA in general, but the cause of this is unknown.

4. Different Porogens

Creating the polymer from Prasad and others (2008) with different a porogen was attempted as it was thought that the polymer synthesis at the high temperature necessary for DMF to boil was too high for vitamin C, which is very heat labile. Furthermore, it was difficult to evaporate DMF at the end of the polymer synthesis because of the high boiling point. Acetonitrile was used as a porogen because it has a similar dipole moment and dielectric constant to DMF. It also has a boiling point of 82°C. However, it was found that the added heat was required for polymerization because at the end of the 4 hours reflux, the monomers did not polymerize and remained in their original condition, undissolved in acetonitrile.

5. Microfluidic chips and C4D

With limited success with polymer synthesis, I was unable to move past this phase and incorporate the polymer into the microfluidic chip. However, I did meet with James Dou, the contact person for Emerging Communication and Technology Institute (ECTI) in Toronto, Canada to talk about the design of the chip. The major parameter of the chips that were changed was creating a thinner base so the barrier between the flow channel and the C4D electrodes is less than 0.5 mm. Furthermore, while trying to obtain a standard curve and optimize the signal for the detection on the C4D, the device had several technical difficulties, requiring it to be sent to the manufacturers for repairs on multiple occasions.